A green chemistry approach towards the stereospecific synthesis of densely-functionalized cyclopropanes via the solid-state photodenitrogenation of crystalline 1-pyrazolines

Trevor Y. Chang, a Daniel M. Adrion, Steven A. Lopez, Miguel A. Garcia-Garibay Miguel A. Garcia-Garibay

^aDepartment of Chemistry and Biochemistry, University of California, Los Angeles, California 90095, United States.

^bDepartment of Chemistry and Chemical Biology, Northeastern University, Boston, Massachusetts 02115, United States.



- Photoproducts feature vicinal quaternary stereocenters
- · Scalability enabled by aqueous crystalline suspensions

ABSTRACT: The cyclopropane ring features prominently in active pharmaceuticals, and this has spurred the development of synthetic methodologies that effectively incorporate this highly-strained motif into such molecules. As such, elegant solutions to prepare densely-functionalized cyclopropanes, particularly ones embedded within the core of complex structures, have become increasingly sought-after. Here we report the stereospecific synthesis of a set of cyclopropanes with vicinal quaternary stereocenters via the solvent-free solid-state photodenitrogenation of crystalline 1-pyrazolines. Density functional theory calculations at the M062X/6-31+G(d,p) level of theory were used to determine the origin of regionselectivity for the synthesis of the 1-pyrazolines; favorable in-phase frontier molecular orbital interactions are responsible for the observation of a single pyrazoline regionsomer. It was also shown that the loss of N_2 may take place via a highly selective solid-state thermal reaction. Scalability of the solid-state photoreaction is enabled through aqueous nanocrystalline suspensions, making this method a "greener" alternative to effectively facilitate the construction of cyclopropane-containing molecular scaffolds.

Introduction

The synthesis of cyclopropyl-containing compounds remains of great importance to the organic chemistry community, as this structurally-unique motif is prevalent in complex natural products, bioactive drug candidates, and extensive sp³rich small-molecule libraries. 1-3 As a result, notable cyclopropanation methodologies, such as nucleophilic or carbenoidmediated additions to double bonds, continue to be developed. 4-12 Recently, the Marek Group described the regio- and diastereoselective synthesis of penta- and hexa-substituted cyclopropanes through copper-catalyzed carbomagnesiation of persubstituted cyclopropenes. ^{13,14} These highly-strained cyclopropenes are well-suited to undergo directed carbometallation reactions with a number of organometallic reagents. The resulting metallated cyclopropanes can be subsequently employed in a variety of useful synthetic transformations that are commonly associated with polysubstituted cyclopropanes. Advances in this field have been incredibly robust, though processes that minimize the use of transition metals or employ more environmentally-benign reagents and solvents remain highly desireable.15

Scheme 1. Photodenitrogenation of 1-pyrazolines towards polysubstituted cyclopropanes.

a). General photodenitrogenation of 1-pyrazolines

Generally poor selectivity resulting from configurationally-labile biradical intermediate 2

$$R_1$$
, R_2 R_2 R_2 R_3 R_4 R_5 R_5 R_6 R_6

· Crystalline reaction cavity improves cyclopropane yields and stereoselectivity

c). This work

$$\begin{array}{c|c} \text{MeO}_2C, & \text{Ar} \\ \hline & \text{N=N} \end{array} \begin{array}{c} \text{Ar} \\ \text{CO}_2R_1 \end{array} \begin{array}{c} \text{h}\nu \\ \text{solid state} \end{array} \begin{array}{c} \text{MeO}_2C, & \text{Ar} \\ \text{CO}_2R_1 \end{array}$$

· Highly stereospecific solid-state synthesis of densely-functionalized cyclopropanes

One attractive alternative is the photochemical denitrogenation of 1-pyrazolines (Scheme 1a). 16-18 Irradiation of pyrazoline 1 generates the corresponding 1,3-biradical intermediate 2 upon double C–N bond homolysis and loss of nitrogen gas. Cyclopropane 3 is subsequently forged via a highly exothermic radical recombination event. While this reaction has been employed in a handful of synthetic endeavors, it remains underutilized in organic synthesis primarily due to a lack of control over the configurationally-labile intermediate 2, often leading to poor yields or loss of stereospecificity. 19

The solid-state photodenitrogenation of crystalline diazoalkanes entails high chemo— and stereoselectivities, primarily a result of the reduced rotational and translational degrees of freedom that reactive intermediates such as **2** are afforded within the crystalline lattice. Our group previously established the quantitative solid-state photodenitrogenation of a series of maleimide-derived pyrazolines. These diazoalkanes were shown to react in the crystalline state, and proceeded with increased reaction stereoselectivities for the corresponding stereoretentive cyclopropanes as compared to their solution-phase counterparts (Scheme 1b). There are additional reports that describe enhanced selectivities in photodenitrogenation reactions of crystalline diazabicyclo[2.2.1]hept-2-ene derivatives; however, there remain relatively limited examples in the literature of this solid-state approach.

To explore the synthetic potential of this reaction, we herein report the synthesis and solid-state photodenitrogenation of a set of crystalline pyrazolines 4 (Scheme 1c). We confirm that the photochemistry is highly stereospecific towards cyclopropanes 5, and that it is scalable to synthetically-useful quantities through the use of aqueous nanocrystalline suspensions. We also report the unexpected observation of a thermal denitrogenation reaction that proceeds with remarkably high stereospecificity in the crystalline state. The resultant cyclopropanes feature vicinal quaternary stereocenters and several orthogonal functional handles such that they are ideal for further synthetic derivatization. ^{25,26} We propose this method as a useful approach to the stereospecifically synthesis of densely-functionalized cyclopropanes with a key step that occurs under conditions that do not employ heavy-metal catalysts nor vola-

tile organic compounds, and anticipate that it may be attractive to the medicinal chemistry community to prepare small, saturated rings within complex architectures.²⁷⁻²⁹

Results and Discussion

Pyrazoline Synthesis and Characterization. Our pyrazoline synthesis commenced from 1-adamantaneacetic acid (not shown) to prepare adamantyl-diazoalkane **6** in multigram quantities (Table 1).³⁰ Acrylates **7a–k** were efficiently obtained either by methylenation of the corresponding aryl acetates or EDCI-mediated coupling of alcohols with atropic acid. Structural variations at the pyrazoline C3 position were achieved though acrylate derivatization. Compounds **7a–f** comprise of a constant –COOMe handle and differ in the aromatic substituent (–Ar), which include *para*-CF₃, -Br, and OMe substituted phenyls, -1-naphthyl, and -3-indole. Compounds **7g–k** all contain an unsubstituted phenyl as –Ar, but instead vary the ester (–COOR₁) substituent (-tBu, -4-pip(NBoc), -Ph, -4-benzophenone, -(1R,2S,5R)-menthyl).

Table 1. Pyrazolines 4a-k synthesized via 1,3-dipolar cycloadditions of diazoalkane 6 with acrylate dipolarophiles 7a-k.

Pyrazoline	Reaction time (h)	Yield ^{a,b} (%)	d.r. (trans : cis)	m.p. ^d (°C)
4a	120	52	2.5:1	97–101
4 b	120	55	2.2:1	117-120
4c	72	55	2.3:1	116-117
4d	144	58	2.4:1	113-114
4e	168	39	3.4:1	109-113
4f	168	29	1.7:1	104-105
4g	72	95	3.7:1	105-106
4h	168	58	3.4:1	114–116

4i	72	83	2.9:1	109-110	
4j	96	95	3.4:1	102-109	
4k	168	68	4.4:1	124-128	
			$d.e.^{c}(2.3:1)$		
		: (1.6:1)			

^aYields are reflective of the pyrazoline diastereomeric mixtures. ^bYields for each derivative generally improve with increased reaction times, though the acrylates are in-turn more susceptible to counterproductive decomposition. $^{c}(R,R)/(S,S)$ and (S,R)/(R,S) diastereomers with respect to chiral menthyl ester. ^dThese pyrazolines are sufficiently high-melting for solid-state photochemical analysis.³⁷

Additionally, the indole and benzophenone groups present in 7f and 7j, respectively, could act as triplet sensitizers as they are known undergo efficient intersystem crossing (ISC) following photochemical excitation. Photodenitrogenation reactions of diazenes that progress through triplet excited-state pathways are known to produce different product distributions compared to ones resulting from direct irradiation and, predominantly, the excited singlet-state manifold.³¹⁻³⁴ With these intermediates in hand, we prepared pyrazolines 4a-k by a regioselective, 1,3-dipolar cycloaddition in yields of 39-97%. While the cycloadditions resulted in a mixture of diastereomers, the major diastereomers were isolated in >99% d.r. as colorless prisms via fractional recrystallization from mixtures of hexanes:diethyl ether.³⁵ It is worth noting that multigram quantities of 4a-k could be obtained through this cycloaddition reaction.³⁶ The methylene -CH₂- resonances in the ¹H NMR spectrum for the major diastereomer 4a were observed as a doublet of doublets at 2.87 and 2.68 ppm with coupling constants of J=13.6 Hz. The ¹H NMR signals corresponding to the same group in the minor diastereomer displayed similar Jvalues, but were instead separated by >1.00 ppm (3.32 and 1.90 ppm). The relative stereochemistry of the major diastereomer 4a was unambiguously confirmed to be trans, both by two-dimensional ¹H NOESY NMR correlations between the methylene protons with either the adamantyl or phenyl moieties and single crystal X-ray diffraction. While this analysis was not carried out for every pyrazoline derivative, the ¹H NMR signals corresponding to both hydrogens for the -CH₂group present in the major diastereomers of the remaining derivatives also fell within a similarly narrow chemical shift range (≈3.00–2.40 ppm) compared to their respective minor diastereomers, implying that the relative stereochemistry of pyrazolines **4b**–**k** was also *trans*.

Single Crystal X-Ray Diffraction of Pyrazoline Reactants. Single X-ray-quality crystals of pyrazolines 4a, 4g, 4i, and 4k were grown from concentrated solutions of either hexanes/diethyl ether (v/v: 1/1, 4a) or diethyl ether (4g, 4i, 4k) via slow evaporation (4a) or storage at -20 °C (4g, 4i, 4k), and structurally analyzed (Figure 1). Compounds 4a, 4g, and 4i crystallized in achiral space groups $P2_1/n$, $Pna2_1$, and $P2_1/c$, respectively, but 4k crystallized in the chiral space group $P2_12_12_1$. Interestingly, 4k, which was synthesized beginning from (IR,2S,5R)-menthol, crystallized as a single enantiomer with (R,R) stereochemistry at the C1 and C3 carbons; all other pyrazoline crystal structures contained racemic mixtures within their respective unit cells. Additionally, the pyrazoline ring in 4k is nearly planar, whereas the -CH₂- carbon puckers out

towards the same side as the adamantyl substituent by $13-20^{\circ}$ in the other derivatives.

It is known that the success of photochemical reactions in the solid-state is highly dependent on the stabilization of the incipient carbon-centered radicals. This is primarily impacted by the dihedral angles formed by the cleaving σ -bond with adjacent π -systems. The greatest amount of stabilization would result from a 90° dihedral that would enable more efficient bond homolysis. Conversely, a 0° dihedral would provide no overlap, disfavoring the photochemical formation of a high-energy biradical intermediate. In pyrazolines 4a, 4g, 4i, and 4k, the dihedral angles formed by the breaking C3–N bond with the –Ar substituents on the same carbon range from 8–60°, while those with the –COOR1 substituent range from \sim 30–45°. We found both of these ranges suitable to exert sufficient π -stabilization to undergo efficient solid-state photodenitrogenation reactions.

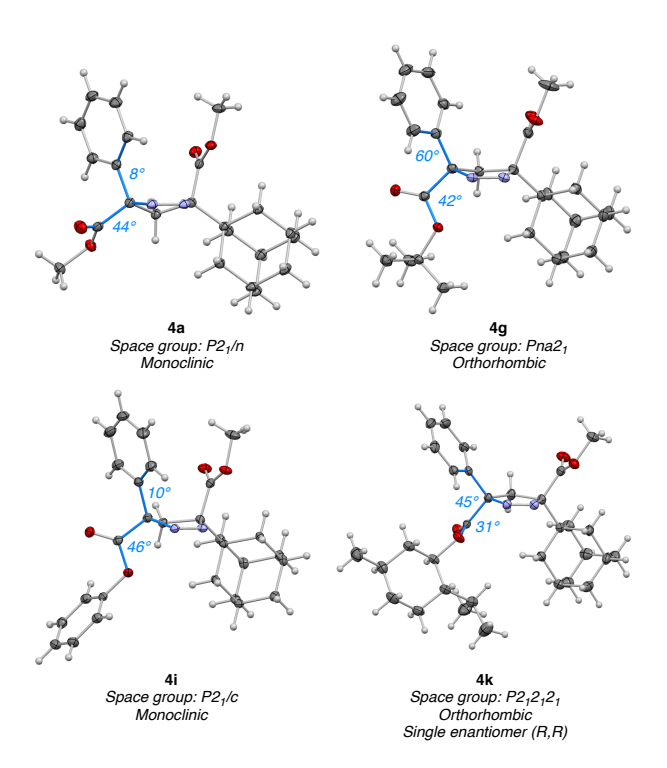


Figure 1. Single crystal X–ray structures of pyrazolines **4a**, **4g**, **4i**, and **4k** with thermal ellipsoids drawn at 50% probability. Carbon-centered radical stabilizing interactions formed by the dihedral angles between breaking σ –bond and neighboring π –systems are highlighted in blue.

Computational Analysis of Cycloaddition Regioselectivity. We computed the transition structures for the cycloaddition of **7a** to **6** to evaluate reactivities (ΔG^{\ddagger}) and regioselectivities ($\Delta \Delta G^{\ddagger}$). The reactants, transition states, and products were optimized in Gaussian 16.⁴⁰ A vibrational analysis was performed on all structures to confirm the presence of a ground state stationary point (zero imaginary frequencies) or a transition structure (one imaginary frequency). The M06-2X/6-31+G(d,p) model chemistry and IEFPCM^{CH2Cl2} solvation model were used for all optimizations.⁴¹⁻⁴³

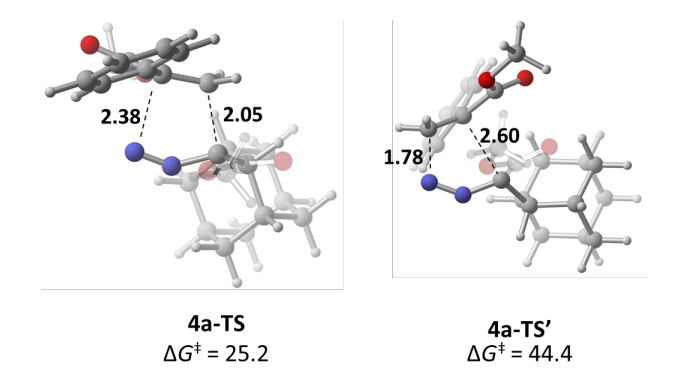


Figure 2. Transition structures **4a-TS** (left) and **4a-TS'** (right) corresponding to the cycloaddition of **6** and **7a**. The dotted lines indicate the forming C–N and C–C bonds. Activation free energies and bond lengths are reported in kcal mol⁻¹ and Angstroms, respectively.

We performed DFT calculations to understand the origin of the complete regioselectivity for the 1,3-dipolar cycloaddition reaction of 6 and 7a. Figure 2 depicts the transition structures 4a-TS and 4a-TS' for pyrazoline 4a. They were shown to have activation free energies of 25.2 and 44.4 kcal mol⁻¹, respectively. A large $\Delta\Delta G^{\ddagger}$ of 19.2 kcal mol⁻¹ agrees with the experimental result of a single regioisomer being formed in the case of 4a. The forming bond distances are 2.38 Å (C-N bond) and 2.05 Å (C-C bond) in 4a-TS. The difference in forming bond lengths is 0.33 Å, indicating an asynchronous transition structure. In 4a-TS', the forming C-N and C-C bonds are 1.78 and 2.60 Å, respectively. The structure of 4a-TS' reveals a considerably more asynchronous bonding than that of 4a-TS (0.82 Å difference in forming bond lengths). The 4a-TS' structure is nearly stepwise because there is no appreciable C-C bond formation. Asynchronous cycloaddition transition structures result from polarized frontier molecular orbitals of the cycloaddends that cause unequal orbital interactions.44-46

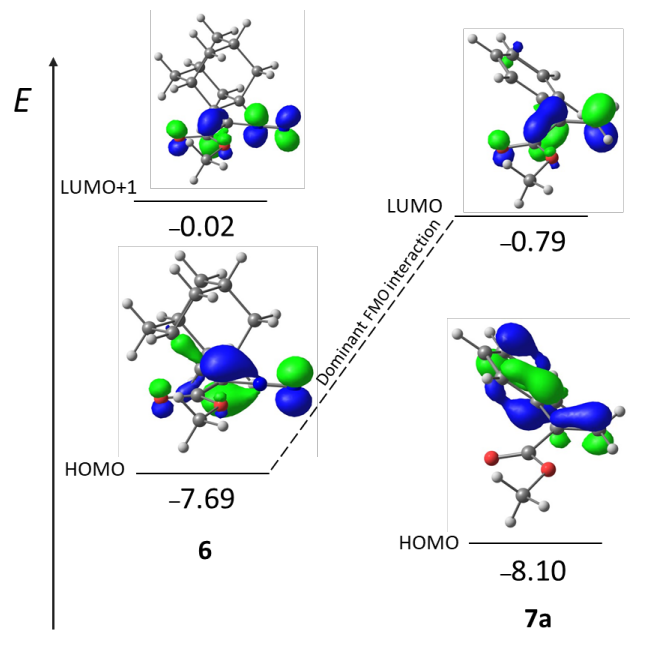


Figure 3. HOMO and LUMO+1 orbitals of the diazoalkane dipole **6** (left) and FMOs of the acrylate dipolarophile **7a** (right).

Orbitals were calculated using the M06-2X/6-31+G(d,p) model chemistry and IEFPCM CH2Cl2. An isovalue of 0.075 was used. Energies are given in eV. The dominant FMO interaction is labeled as $HOMO_{dipole} - LUMO_{dipolarophile}$.

We computed the frontier molecular orbitals (FMOs) involved in the cycloaddition of 6 to 7a to visualize this effect and understand how the orbitals affect the ΔG^{\ddagger} (Figure 3). The HOMO (π -orbital) of 6 has an energy of -7.69 eV and is polarized towards the C-terminus; the LUMO+1 (π^* -orbital) of 6 has an energy of -0.02 eV and is also polarized towards the Cterminus. The HOMO of 7a has an energy of -8.10 eV and is polarized towards the methylene-terminus; the LUMO (π^* orbital) of 7a has an energy of -0.79 eV. The dominant frontier molecular orbital (FMO) interaction for the cycloaddition of 6 and 7a involves the HOMO of the dipole (6) overlapping with the LUMO of the dipolarophile (7a); the energy difference between these orbitals is 6.90 eV. When the atoms with larger orbital coefficients are matched in 4a-TS, there is a stronger stabilizing FMO interaction in the transition state, resulting in a lower ΔG^{\ddagger} (25.2 kcal mol⁻¹). When the termini with the larger orbital coefficients are mismatched, the FMO interactions are substantially weaker. This effect increases the energy of 4a-TS' and is responsible for the observed complete regioselectivity.

Solution Photochemistry. With the crystalline pyrazolines 4a-k in hand, we set out to explore the photodenitrogenative cyclopropanation reaction. Photochemical reactions in solution were carried out in degassed benzene- d_6 using a medium-pressure Hg Hanovia lamp equipped with a Pyrex filter (>290 nm). Each derivative was irradiated to complete conversion within 25 min (determined by ¹H NMR analysis of the pyrazoline -CH₂- signals). These reactions proceeded moderately well for cyclopropanes 5a-k (Table 2). Cyclopropane stereoselectivities were determined by ¹H NMR integration of clean cyclopropane signals for either the -CH₂- (ca. 2.40–2.00 ppm) or –COOMe (ca. 3.20 ppm) groups. The good retention of stereochemistry observed was likely due to the presumed singlet-state nature of the 1,3-biradical and the close proximity of the incipient carbon radicals, which would lead to a rapid recombination event and minimal formation of stereoinverted cyclopropanes 8a-k that would result from C-C bond rotation prior to recombination.

Table 2. Stereoselectivities for cyclopropanes 5a-k upon irradiation of pyrazolines 4a-k in solution and as dry, crystalline powders.

$$\begin{array}{c} \text{MeO}_2\text{C}, & \text{Ar} \\ \text{Ad} & \text{N=N} \\ \end{array} \\ \begin{array}{c} \text{Ad} & \text{CO}_2\text{R}_1 \\ \end{array} \\ \begin{array}{c} \text{Ad} & \text{N=N} \\ \end{array} \\ \begin{array}{c} \text{Ad} & \text{CO}_2\text{R}_1 \\ \end{array} \\ \begin{array}{c} \text{Ad} & \text{N=N} \\ \end{array} \\ \begin{array}{c} \text{Ad} & \text{CO}_2\text{R}_1 \\ \end{array} \\ \begin{array}{c} \text{Ad} & \text{N=N} \\ \end{array} \\ \begin{array}{c} \text{Solution: 2.0 mg / 0.5 mL C}_6D_6 \\ \text{Solid state: 2.0 mg crushed powder} \end{array} \\ \begin{array}{c} \text{MeO}_2\text{C}, & \text{N=N} \\ \end{array} \\ \begin{array}{c} \text{Ad} & \text{CO}_2\text{Me} \\ \end{array} \\ \begin{array}{c} \text{Ad} &$$

Entry	Time ^a (min)	Solution ^{b,c} (%)	Solid- state ^c (%)	m.p. (°C)
5a	10	77	97	111–113
5b	20	83	99	183-184
5c	15	79	98	188-189
5d	15	80	88	134–135
5e	10	81	91	$187 - 196^d$
5f	15	77	>99	59–63
5g	25	83	96	100-102
5h	10	74	93	139-142
5i	10	82	99	84–87
5j	10	77	>99	125-127
5k	15	>99	>99	150-154

^aIdentical irradiation times for solution and solid-state samples. $^b100\%$ starting material conversion. ^cTrace vinyl resonances that correspond to 1,2-H shift products, which result from a 1,3-biradical intermediate, are visible in the crude 1 H NMR spectra (ca. 6.00–4.50 ppm). ^dInseparable mixture of diastereomers **5e** and **8e**.

Photochemical Reactions in Crystalline Solids. Following investigation of the solution-phase reactivity, we turned our attention to the solid-state photodenitrogenation reactions. Crystalline samples (ca. 2 mg) were ground into a thin, transparent layer on microscope slides and irradiated for identical times as the solution experiments, typically proceeding with >95% conversion. When 4a–k were irradiated as bulk powders, the stereoselectivities for 5a–k greatly improved relative to the corresponding solution-phase irradiations; these values ranged from 88–99% (Figure 4). Electronic variation in the –

Ar substituents across pyrazolines **4a**—f had minimal impact on the resultant cyclopropane stereoselectivities (88–99%). Similarly, reactions of pyrazolines **4g**—k were minimally affected by ester substituents featuring varied degrees of steric bulk, displaying minor stereoselectivity differences between 93–99% for **5g**—k. These solid-state photodenitrogenation reactions may be classified as "topochemical" considering that photoproducts **5a**—k are expected to follow the "least-motion" descriptor put forth by Schmidt et al. in 1971.⁴⁷

Single Crystal X-Ray Diffraction of Cyclopropane Photoproducts. Single crystal X-ray structure elucidation was again carried out on colorless prism crystals of cyclopropanes 5a and 5k grown from solutions of hexanes:diethyl ether (Figure 4a). 48 Analysis of both crystal structures confirmed the relative stereochemistry of the major photodenitrogenation product to be trans, therefore confirming that the stereochemistry set in the corresponding pyrazolines is highly preserved throughout the solid-state reactions. Cyclopropane 5a crystallized in the monoclinic space group P2₁/c, which differs from the corresponding pyrazoline 4a (P2₁/n) only by the axis of the glide plane symmetry operations. Here, the -COOMe carbonyls are now both oriented in the direction of the cyclopropane methylene, meaning the carbonyl at the C3 position underwent a significant 146° rotation towards the -CH₂- from the position observed in the crystal structure of **4a**. The crystal structure for 5k revealed a single enantiomer (S,S), and crystallized in the achiral space group P1. The ester carbonyls are now oriented opposite from the methylene, resulting from >100° rotations from their starting orientations towards the pyrazoline -CH₂- in 4k.

Interestingly, the newly-forged C–C cyclopropane bonds in both structures are of longer lengths that would be expected for both unsubstituted cyclopropanes (1.51 Å) and typical C(sp³)–C(sp³) bonds (1.54 Å).⁴⁹ These bonds are unusually long, even greater than the 1.54 Å experimentally observed in crystalline donor-acceptor cyclopropanes.⁵⁰ This is presumably due to the steric bulk of the vicinal quaternary centers; this feature is more clearly illustrated when viewing the space-fill model for **5a** and highlights the density of this motif within the cyclopropane rings (Figure 4b).

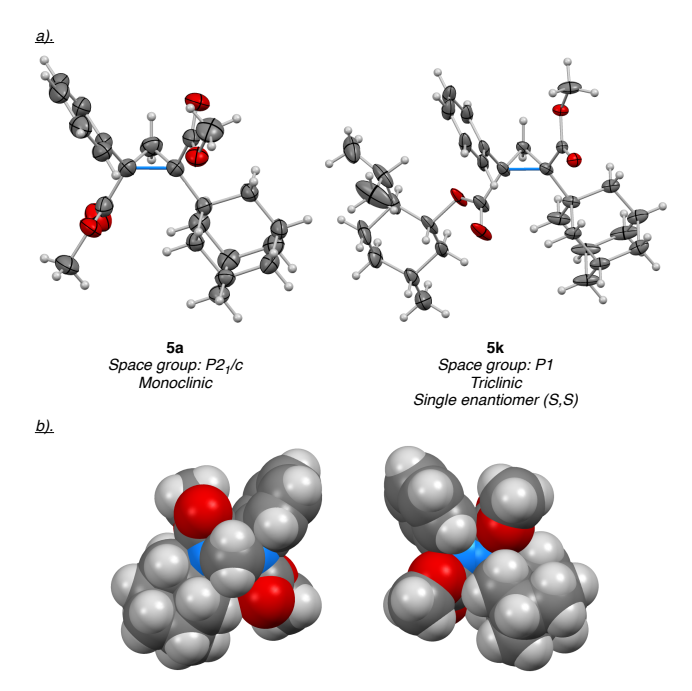


Figure 4. a). Single crystal x–ray structures of cyclopropanes **5a** and **5k** with thermal ellipsoids drawn at 50% probability. Longer cyclopropane C–C bonds in **5a** (1.557(2) Å) and **5k** (1.546(3) Å) highlighted in blue. b). Single crystal x–ray structure of **5a** depicted as space-fill model with vicinal quaternary stereocenters colored in blue.

Scaling Up Reactions in Crystalline Solids. Both starting material conversion and reaction scalability are a challenge when samples 4a-k are irradiated as neat polycrystalline powders on >10 mg samples due to limited light penetration into the bulk material. This was overcome by irradiating the pyrazolines as aqueous nanocrystalline suspensions (Figure 5). Our group has previously demonstrated that irradiating organic crystals prepared in this manner greatly minimizes optical issues associated with irradiation of dry powders.^{51–54} These suspensions can also be run through flow reactors, allowing for irradiation of crystalline material on scales as large as 25 g. Solid-state photodenitrogenations of pyrazolines 4c, 4h, and 4i were carried out under such conditions to high conversions (>90%) on scales as large as 200 mg. The stereoselectivities for the corresponding cyclopropanes 5c, 5h, and 5i observed in these reactions were comparable to the results from the bulk-powder irradiations, and the yields greatly improved when compared to their solution-phase counterparts, as seen by the >100% increase for **5h**. 55,56 These results demonstrate that the preparation and subsequent irradiation of suspended crystalline samples is an effective method to carry out highlyselective solid-state photochemical reactions on syntheticallyuseful scales.

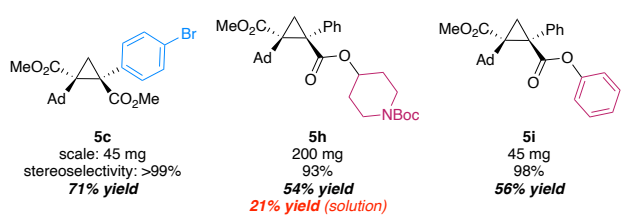


Figure 5. Results of the photochemical reactions for **5c**, **5h** and **5i** using nanocrystalline suspensions of the corresponding pyra-

zolines. Detailed suspension preparation conditions can be found in the experimental section below.

Thermal Denitrogenation in the Crystalline Solid-State. During melting point characterization of 4a-k, we noticed that each event was accompanied by visible bubble formation while the crystal specimens remained largely intact. Further analysis of these samples on larger scales revealed that thermal denitrogenation and cyclopropanation was occurring around the melting point temperatures, and the bubbling was presumably due to nitrogen gas escaping from the crystals.⁵⁷ A crystal of 4k, which has a melting point of 124-128 °C, was heated at 110 °C and monitored via an optical microscope equipped with a camera (see SI for video). Still images from the movie highlight the formation and movement of several bubbles, one of which is tracked by the red circle (Figure 6). Based on this observation, it was of interest to determine whether or not the thermal reaction stereoselectivities would be comparable to those observed in the photochemical experiments. To our delight, when 4h was heated as a dry powder, **5h** was observed in 94% selectivity (Table 3). Differential scanning calorimetric (DSC) analysis of 4h displayed a sharp exothermic event occurring around 115 °C that matched the temperature at which this derivative was seen to melt at (SI page S8).

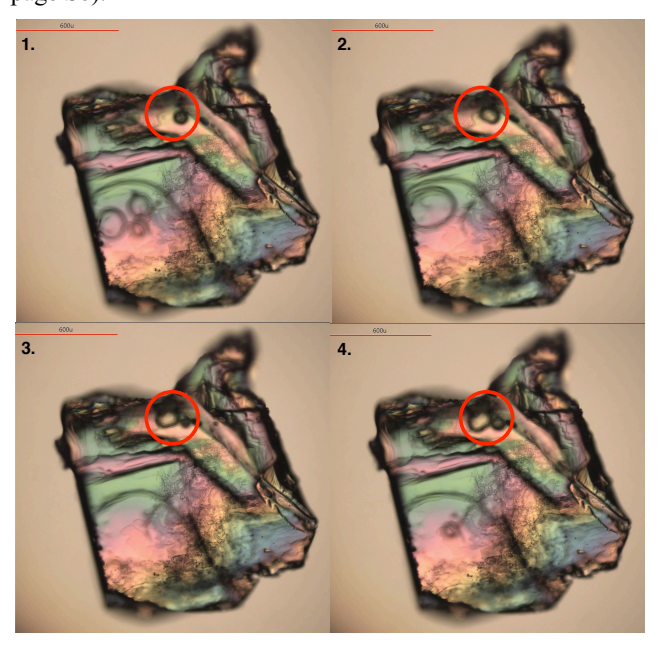


Figure 6. Crystal of pyrazoline **4k** heated at 110 °C. Still movie images 1–4 were captured using a polarizing microscope and show the movement of a bubble, circled in red, every 10 ms; this is presumably due to thermally-induced nitrogen expulsion.

Additional DSC data for **4h** collected with an isothermal run at 95 °C, however, revealed a much broader exothermic peak, which was correlated with thermogravimetric analysis (TGA) data to be the loss of N_2 (SI page S9). This suggested that the thermal denitrogenation of these pyrazolines occurs within the crystal environment, and the observed melting for the pyrazoline samples may instead be the result of the change in the chemical composition of the crystalline solid. This represents a rare example of a solid-state thermal reaction, and suggests further development of mechanochemically-responsive organic crystals. $^{58-60}$

Table 3. Cyclopropane 5h stereoselectivities for photochemical and thermal denitrogenation of 4h.

Reaction	5h (%)	5h (%)
medium ^a	hv (> 290 nm)	Δ (120 °C)
Solution	74	87
Solid state	93	94

^aSolution photolyses were carried out in benzene- d_6 , solution thermolyses were carried out in toluene, and solid-state samples were reacted as dry powders.

Conclusions

In summary, we have shown the stereospecific synthesis of a set of vicinal quaternary center-containing cyclopropanes via the solid-state photodenitrogenation of the corresponding crystalline 1-pyrazolines. The cyclopropane stereoselectivities demonstrate marked improvements following irradiation in the solid state as compared to the results obtained in solution. We also showed that these photodenitrogenation reactions are effectively scalable through the use of aqueous crystalline suspensions, proceeding with good yields and high stereoselectivities. Interestingly, the thermal denitrogenation of these pyrazolines appears to occur within a well-maintained crystalline lattice, resulting in excellent cyclopropane stereoselectivities that are comparable to the solid-state photodenitrogenation reactions. We propose that the solid-state photochemical approach described in this manuscript holds promise as an effective green chemistry tool to facilitate access to highly-strained, complex structural motifs sans heavy-metal catalysts and volatile organic compounds.

Experimental Section

Materials and Methods. All chemicals were purchased from commercial suppliers and used as received. Tetrahydrofuran (THF) was distilled over sodium/benzophenone. Dichloromethane (DCM) was distilled over calcium hydride. All other solvents used as received. Reactions at -78 °C were carried out in acetone-dry ice baths, reactions at 0 °C were carried out in water-ice baths, room temperature reactions were carried out between 20-25 °C, and reactions at elevated temperatures were carried out in oil baths or aluminum heating blocks. Sample irradiations for photochemical reactions were performed in Pyrex glassware contained within a photochemical reactor equipped with a Hanovia 450 W medium-pressure mercury vapor UV lamp, which was seated in a water-cooled quartz immersion well. Analytical thin-layer chromatography (TLC) was performed using precoated TLC plates with Silica Gel 60 F254 and visualized using combinations of UV and appropriate staining as specified. Flash column chromatography was performed using silica gel (230-400 mesh) as the stationary phase. ¹H and ¹³C{¹H} NMR spectra for characterization of synthetic targets were recorded on a Bruker Avance spectrometer at 500 or 600 MHz (1 H) and 126 MHz (13 C(1 H)). All chemical shifts are reported in ppm on the δ -scale relative

to residual solvent signals as reference (CDCl₃ δ 7.26 for ¹H and δ 77.16 for ¹³C; C₆D₆ δ 7.16 for ¹H and δ 128.06 for ¹³C, $(CD_3)_2CO \delta 2.05$ for ¹H and $\delta 29.84$ for ¹³C). Multiplicities are reported as singlet (s), doublet (d), triplet (t), quartet (q), quintet (quint), septet (sep), and multiplet (m). IR spectral data were obtained using an Attenuated Total Reflectance (ATR) spectrometer as the neat compound and values are reported in cm⁻¹. High-resolution mass spectrometry data was collected using a Direct Analysis in Real Time Ionization technique with a QExactive Plus Hybrid Quadrupole-Orbitrap mass spectrometer in positive ion mode. Melting point values were recorded on a Melt-Point II® apparatus. Differential Scanning Calorimetry (DSC) data were recorded on a Mettler Toledo 3+ DSC under a nitrogen atmosphere. Thermogravimetric analysis (TGA) data were recorded on a Perkin Elmer Diamond Thermogravimetric Differential Thermal Analyzer with the following sequence: 1). Hold 50 °C for 1.0 min 2). Heat 50 \rightarrow 85 °C at 5 °C/min 3). Hold 85 °C for 15.0 min 4). Heat 85 \rightarrow 90 °C at 5 °C/min 5). Hold 90 °C for 30.0 min 6). Heat 90 \rightarrow 95 °C at 5 °C/min 7). Hold 95 °C for 30.0 min 8). Heat 95 \rightarrow 100 °C at 5 °C/min 9). Hold 100 °C for 15.0 min. Singlecrystal X-ray diffraction data were collected on a Bruker Smart ApexII CCD single-crystal X-ray diffractometer. Single X-ray-quality crystals of compounds 4a, 5a, 4g, 4i, 4k, and 5k were grown from concentrated solutions of either hexanes/diethyl ether (v/v: 1/1, 4a, 5a) or diethyl ether via slow evaporation (4a, 5a, 5k) or storage at -20 °C (4g, 4i, 4k). Thermal denitrogenation videos were captured on a Nikon ECLIPSE LV100N-CH POL microscope equipped with a Linkam LNP96 liquid nitrogen cooling system and a frontmounted camera + Link image capture module upgrade (L-PG32C-LINKOP-PKG) from McCrone Microscopes and Ac-

Synthesis of diazoalkane 6: Carried out according to a previously reported procedure with minor modifications.³⁰

- (9) Methyl 2-((3r,5r,7r)-adamantan-1-yl)acetate. 1-adamantaneacetic acid (3.00 g, 15.4 mmol) was dissolved in 30.0 mL methanol in a 100 mL roundbottom flask. Concentrated $\rm H_2SO_4$ (0.8 mL, 15.4 mmol) was added neat, and the reaction was heated at 65 °C for 22 h. The reaction was then cooled to room temperature, slowly poured into 20.0 mL of saturated aqueous NaHCO₃, and carefully neutralized until the aqueous layer reached pH > 7. Organics were extracted with CH₂Cl₂ (3 x 20.0 mL), dried over Na₂SO₄, and concentrated under rotary evaporation to afford **9** as a clear, colorless oil (3.17 g, 98% yield). $\rm R_f = 0.52$ (9:1 hexanes/ethyl acetate). Spectral data match those previously reported.³⁰
- Methvl 2-((3r,5r,7r)-adamantan-1-yl)-3oxopropanoate. Reaction carried out under Argon. 9 (2.00 g, 9.6 mmol) was dissolved in 10.0 mL dry THF and added dropwise to freshly-made LDA (1.6 equiv, 15.4 mmol) in 45.0 mL THF at -78 °C in a flame-dried 250 mL roundbottom flask. Reaction was stirred for 90 min, then ethyl formate (0.93 mL, 11.5 mmol) in 4.0 mL THF was added. The resulting pale-yellow solution was stirred for an additional 2 h at – 78 °C. After 2 h, several small ice cubes were added to the reaction mixture, then the entire solution was poured into 20.0 mL of ice water. This solution was allowed to warm up to room temperature, then extracted with EtOAc (3 x 20.0 mL), washed with brine (1 x 20.0 mL), dried over Na₂SO₄, and concentrated directly onto silica gel (5 g) under rotary evaporation. Purification via flash column chromatography (35 g silica

gel, 19:1 hexanes/ethyl acetate) afforded **10** as a colorless solid (1.7 g, 75% yield). R_f = 0.17 (19:1 hexanes/ethyl acetate). Spectral data match those previously reported.³⁰

(6) *Methyl 2-((3r,5r,7r)-adamantan-1-yl)-2-diazoacetate.* Reaction carried out under Argon. 10 (1.25 g, 5.29 mmol) was dissolved in 35.0 mL THF in flame-dried 100 mL roundbottom flask and cooled to 0 °C. 1,8-Diazabicyclo[5.4.0]undec-7ene (DBU) (1.18 mL, 7.93 mmol) was added neat via syringe, stirred for 40 and reaction was min. acetamidobenzenesulfonyl azide (p-ABSA) (1.91 g, 7.93 mmol) in 20.0 mL THF was added via syringe, and resulting yellow solution was allowed to warm to room temperature while stirring for 18 h. Upon completion, 2.0 mL of saturated aqueous NH₄Cl was added, then poured into 20.0 mL of H₂O. Organics were extracted with CH₂Cl₂ (3 x 20.0 mL), dried over Na₂SO₄, and concentrated directly onto silica gel (10 g) under rotary evaporation. Purification via flash column chromatography (35 g silica gel, 50:1 hexanes/ethyl acetate) afforded **6** as a yellow solid (1.3 g, 92% yield). $R_f = 0.43$ (19:1 hexanes/ethyl acetate). Spectral data match those previously reported.³⁰ (Notes: Conversion of 1-adamantaneacetic acid can be monitored via TLC via bromocresol green stain. Formylated 10 can be visualized on TLC via KMnO₄ stain. 6 is an unusually stable α-diazoalkane and unlikely to pose notable explosive hazards; nonetheless, caution is still recommended.)

General Procedure for Acrylate Synthesis (Note: All others were synthesized according to previously reported procedures^{61,62} via the corresponding aryl acetates **11a–g**.

Reactions carried out under Argon. Atropic acid (1.0 equiv), the corresponding alcohol (1.0 equiv), and 3-(((ethylimino)methylene)amino)-N,N-dimethylpropan-1amine•HCl (EDCI•HCl) (1.1 equiv) were dissolved in dry DCM (0.1 M with respect to (wrt) atropic acid) in a flamedried roundbottom flask. 4-dimethylaminopyridine (DMAP) (0.5 equiv) was added in CH₂Cl₂ (0.17 M) in one portion, and the reaction was stirred at room temperature for 22 h. Crude solution was diluted with Et2O, then washed with saturated aqueous NH₄Cl (2x), saturated aqueous NaHCO₃ (3x), brine (1x), dried over Na₂SO₄, and concentrated directly onto silica gel. Purification via flash column chromatography (19:1 hexanes/ethyl acetate) afforded the corresponding acrylates as white solids. (Note: All acrylates should be stored at 0 °C neat or in benzene, if they are not to be used within 10 h of isolation, to minimize decomposition.)

- (7h) Tert-butyl 4-((2-phenylacryloyl)oxy)piperidine-1-carboxylate. (3.13 g, 70% yield). Colorless solid. $R_f = 0.34$ (9:1 hexanes/ethyl acetate). 1H NMR (600 MHz, CDCl₃) δ : 7.89 (m, 2H), 7.81 (m, 2H), 7.61 (m, 1H), 7.53-7.47 (m, 4H), 7.43-7.38 (m, 3H), 7.32 (m, 2H), 6.66 (d, J = 0.8 Hz, 1H), 6.14 (d, J = 0.8 Hz, 1H); $^{13}C\{^1H\}$ NMR (126 MHz, CDCl₃) δ : 195.7, 164.8, 154.2, 140.6, 137.6, 136.2, 135.3, 132.6, 131.8, 130.1, 129.3, 128.7, 128.52, 128.49, 128.4, 121.7; IR (powder) v/cm^{-1} 3285 (w), 3038 (w), 2922 (w), 2068 (w), 1979 (w), 1908 (w), 1823 (w), 1734 (m), 1648 (m), 1595 (m), 1497 (m), 1446 (m), 1280 (m), 1168 (m), 1068 (m), 923 (m), 858 (m), 780 (m), 692 (s); HRMS (APCI) m/z: [M + H]+ calc. for $C_{22}H_{17}O_3+$, 329.1172, found 329.1160; mp: 85-87 $^{\circ}C$.
- (7j) 4-benzoylphenyl 2-phenylacrylate. (542 mg, 61% yield). Colorless solid. $R_f = 0.34$ (9:1 hexanes/ethyl acetate).

 ¹H NMR (600 MHz, CDCl₃) δ : 7.89 (m, 2H), 7.81 (m, 2H), 7.61 (m, 1H), 7.53-7.47 (m, 4H), 7.43-7.38 (m, 3H), 7.32 (m, 2H), 6.66 (d, J = 0.8 Hz, 1H), 6.14 (d, J = 0.8 Hz, 1H);

 $^{13}C\{^{1}H\}$ NMR (126 MHz, CDCl₃) δ : 195.7, 164.8, 154.2, 140.6, 137.6, 136.2, 135.3, 132.6, 131.8, 130.1, 129.3, 128.7, 128.52, 128.49, 128.4, 121.7; IR (powder) ν/cm^{-1} 3285 (w), 3038 (w), 2922 (w), 2068 (w), 1979 (w), 1908 (w), 1823 (w), 1734 (m), 1648 (m), 1595 (m), 1497 (m), 1446 (m), 1280 (m), 1168 (m), 1068 (m), 923 (m), 858 (m), 780 (m), 692 (s); HRMS (APCI) m/z: [M + H]+ calc. for $C_{22}H_{17}O_{3}+$, 329.1172, found 329.1160; mp: 85-87 °C.

(7k) (1R,2S,5R)-2-isopropyl-5-methylcyclohexyl 2-phenylacrylate (380 mg, 39% yield). Colorless solid. R_f = 0.75 (9:1 hexanes/ethyl acetate). ¹H NMR (500 MHz, CDCl₃) δ: 7.43-7.40 (m, 2H), 7.37-7.30 (m, 3H), 6.29 (d, J = 1.3 Hz, 1H), 5.87 (d, J = 1.3 Hz, 1H), 4.87 (dt, J = 4.4, 10.9 Hz, 1H), 2.14-2.07 (m, 1H), 1.94 (dquint, J = 2.7, 7.0, 1H), 1.73-1.66 (m, 2H), 1.58-1.49 (m, 1H), 1.48-1.40 (m, 1H), 1.15-1.01 (m, 2H), 0.93 (d, J = 6.6 Hz, 3H), 0.90 (d, J = 7.0 Hz, 3H), 0.80 (d, J = 7.0 Hz, 3H); 13 C{ 1 H} NMR (126 MHz, CDCl₃) δ: 166.6, 142.1, 137.0, 128.4, 128.19, 128.18, 125.9, 75.2, 47.2, 40.9, 34.4, 31.6, 26.5, 23.6, 22.2, 20.9, 16.5; IR (film) v/cm⁻¹ 3084 (w), 2954 (m), 2859 (m), 1713 (s), 1614 (w), 1446 (m), 1192 (s), 1179 (s), 1090 (m), 774 (m), 698 (s); HRMS (APCI) m/z: [M + H]+ calc. for C₁₉H₂₇O₂+, 287.2006, found 287.2010; mp: 44-46 °C.

General Procedure for 1,3-Dipolar Cycloadditions Diazoalkane 6 (1.0 equiv) and the corresponding acrylate 7a-k (2.0 equiv) were dissolved in CH₂Cl₂ (0.8 M wrt 6) in 1 dram vials and stirred at ambient temperatures for at least 72 h. The crude reactions were then concentrated directly onto silica gel. Purification via flash column chromatography, followed by recrystallization (minimal 1:1 hexanes/diethyl ether stored at 0 °C for 3 days (two cycles), 100% diethyl ether (one cycle)) afforded diastereomerically pure pyrazolines 4a-k. (Notes: Yields improve if reaction stirred for longer than 72 h, though acrylate decomposition complicates chromatography. Pyrazolines should be exposed to minimal light and stored at 0 °C, as non-specific and incomplete denitrogenation is likely to occur. Minimal amounts of CH2Cl2 can be added if samples will not dissolve in appropriate crystallization solvent. The first crystallization cycle mother liquors are enriched in the major, trans pyrazoline diastereomer; these samples were concentrated via rotary evaporation and resubjected to conditions listed above. Precipitated solids, typically enriched in the cis pyrazolines, can be treated in the same manner for further resolution.)

Characterization Data for Pyrazolines 4a-k

- (4a) Dimethyl (3R,5R)-3-((3R,5R,7R)-adamantan-1-yl)-5-phenyl-4,5-dihydro-3H-pyrazole-3,5-dicarboxylate. (35 mg, 52% yield). Colorless solid. $R_f = 0.11$ (19:1 hexanes/ethyl acetate). 1H NMR (500 MHz, C_6D_6) δ : 7.44-7.42 (m, 2H), 7.02-7.00 (m, 2H), 6.95-6.92 (m, 1H), 3.28 (s, 3H), 2.96 (s, 3H), 2.87 (d, J = 13.6 Hz, 1H), 2.68 (d, J = 13.6 Hz, 1H), 2.21-2.16 (m, 3H), 1.88 (m, 3H), 1.69-1.63 (m, 3H), 1.56-1.53 (m, 6H); $^{13}C\{^1H\}$ NMR (126 MHz, C_6D_6) δ : 170.7, 170.7,137.8, 128.7, 128.3, 125.9, 105.7, 100.4, 53.5, 51.9, 38.9, 37.3, 36.7, 32.7, 28.4; IR (powder) ν/cm^{-1} 3057 (w), 2909 (m), 2849 (m), 1741 (s), 1722 (s), 1558 (w), 1446 (m), 1438 (m), 1237 (s), 1089 (m), 765 (w), 694 (w); HRMS (APCI) m/z: [M + H]+ calc. for $C_{23}H_{29}N_2O_4$ +, 397.2122, found 397.2116; mp: 97-101 °C.
- **(4b)** *Dimethyl* (3R,5R)-3-((3R,5R,7R)-adamantan-1-yl)-5-(4-(trifluoromethyl)phenyl)-4,5-dihydro-3H-pyrazole-3,5-

- *dicarboxylate*. (23 mg, 55% yield). Colorless solid. $R_f = 0.30$ (9:1 hexanes/ethyl acetate). 1H NMR (500 MHz, C_6D_6) δ: 7.32 (d, J = 8.2 Hz, 2H), 7.23 (d, J = 8.2 Hz, 2H), 3.27 (s, 3H), 2.89 (s, 3H), 2.82 (dd, J = 13.8, 0.8 Hz, 1H), 2.53 (d, J = 13.8 Hz, 1H), 2.18-2.11 (m, 3H), 1.88 (m, 3H), 1.66-1.60 (m, 3H), 1.59-1.50 (m, 6H); $^{13}C\{^1H\}$ NMR (126 MHz, CDCl₃) δ: 170.5, 170.0, 141.6, 131.0 (q, J = 32.9 Hz), 127.2 (q, J = 272.2 Hz), 126.6, 125.7 (q, J = 3.7 Hz), 106.3, 100.0, 53.8, 52.1, 39.0, 37.3, 36.7, 32.6, 28.4; IR (powder) ν/cm⁻¹ 3078 (w), 2913 (m), 2857 (m), 1735 (s), 1722 (s), 1619 (w), 1550 (w), 1448 (m), 1437 (m), 1329 (s), 1124 (s), 1110 (s), 847 (m), 792 (m), 719 (w); HRMS (APCI) m/z: [M + H]+ calc. for $C_{24}H_{28}F_3N_2O_4+$, 465.1996, found 465.2005; mp: 117-120 °C.
- (4c) Dimethyl (3R,5R)-3-((3R,5R,7R)-adamantan-1-yl)-5-(4-bromophenyl)-4,5-dihydro-3H-pyrazole-3,5-dicarboxylate. (21 mg, 55% yield). Colorless solid. $R_f=0.13$ (9:1 hexanes/ethyl acetate). ¹H NMR (500 MHz, CDCl₃) δ : 7.45-7.42 (m, 2H), 7.15-7.12 (m, 2H), 3.81 (s, 3H), 3.40 (s, 3H), 2.59 (d, J=13.8 Hz, 1H), 2.42 (d, J=13.8 Hz, 1H), 2.05 (m, 3H), 1.97-1.91 (m, 3H), 1.75-1.64 (m, 6H), 1.55-1.49 (m, 3H); 13 C{ 1 H} NMR (126 MHz, CDCl₃) δ : 170.6, 170.2, 136.7, 131.9, 127.8, 122.7, 106.1, 99.8, 53.7, 52.1, 38.9, 37.3, 36.7, 32.5, 28.4; IR (powder) v/cm⁻¹ 3069 (w), 2914 (m), 2851 (m), 1731 (s), 1590 (w), 1557 (w), 1484 (m), 1449 (m), 1252 (s), 1114 (m), 1008 (m), 828 (m), 788 (m), 727 (m); HRMS (APCI) m/z: [M + H]+ calc. for $C_{23}H_{28}BrN_2O_4+$, 475.1222, found 475.1240; mp: 116-117 °C.
- (4d) Dimethyl (3R,5R)-3-((3R,5R,7R)-adamantan-1-yl)-5-(4-methoxyphenyl)-4,5-dihydro-3H-pyrazole-3,5-dicarboxylate. (58 mg, 58% yield). Colorless solid. $R_f = 0.20$ (17:3 hexanes/ethyl acetate). ¹H NMR (600 MHz, CDCl₃) δ: 7.18 (m, 2H), 6.82 (m, 2H), 3.80 (s, 3H), 3.77 (s, 3H), 3.38 (s, 3H), 2.54 (d, J = 13.7 Hz, 1H), 2.46 (d, J = 13.7 Hz, 1H), 2.04 (m, 3H), 1.97-1.90 (m, 3H), 1.75-1.64 (m, 6H), 1.56-1.50 (m, 3H); ¹³C {¹H} NMR (126 MHz, CDCl₃) δ: 170.8, 170.7, 159.3, 129.5, 127.1, 113.9, 105.4, 99.7, 55.2, 53.3, 38.7, 37.2, 36.6, 32.5, 28.3; IR (film) ν/cm⁻¹ 3004 (w), 2907 (m), 2852 (m), 1732 (s), 1609 (w), 1582 (w), 1512 (m), 1455 (m), 1250 (s) 1184 (m), 832 (w), 790 (w), 718 (w); HRMS (APCI) m/z: [M + H]+ calc. for $C_{24}H_{31}N_2O_5+$, 427.2228, found 427.2216; mp: 113-114 °C.
- (4e) Dimethyl (3R,5R)-3-((3R,5R,7R)-adamantan-1-yl)-5-(naphthalen-1-yl)-4,5-dihydro-3H-pyrazole-3,5-dicarboxylate. (94 mg, 39% yield). Colorless solid. $R_f = 0.37$ (17:3 hexanes/ethyl acetate). ¹H NMR (600 MHz, CDCl₃) δ: 7.88-7.84 (m, 1H), 7.78 (d, J = 8.3 Hz, 1H), 7.75-7.72 (m, 1H), 7.50 (m, 2H), 7.33 (dd, J = 8.2, 7.3 Hz, 1H), 7.06 (dd, J = 7.3, 1.1 Hz, 1H) 3.73 (s, 3H), 3.39 (s, 3H), 3.17 (d, J = 13.3 Hz, 1H), 2.38 (d, J = 13.3 Hz, 1H), 2.07-2.01 (m, 6H), 1.77-1.68 (m, 6H),1.58 (m, 3H); ${}^{13}C\{{}^{1}H\}$ NMR (126 MHz, CDCl₃) δ : 171.1, 170.7, 134.9, 134.8, 130.6, 129.8, 129.3, 127.0, 126.0, 125.1, 123.9, 123.85, 107.5, 101.5, 53.1, 51.3, 39.3, 37.8, 36.9, 33.4, 28.8; IR (powder) v/cm⁻¹ 3055 (w), 2914 (m), 2852 (m), 1732 (s), 1721 (s), 1596 (w), 1542 (w), 1509 (w), 1436 (m), 1250 (s) 1098 (m), 800 (m), 793 (m), 779 (s), 665 (w); HRMS (APCI) m/z: [M + H]+ calc. for $C_{27}H_{31}N_2O_4$ +, 447.2278, found 447.2262; mp: 109-113 °C.
- **(4f)** Dimethyl (3R,5R)-3-((3R,5R,7R)-adamantan-1-yl)-5-(1-(tert-butoxycarbonyl)-1H-indol-3-yl)-4,5-dihydro-3H-pyrazole-3,5-dicarboxylate. (20 mg, 29% yield). Colorless solid. $R_f = 0.18$ (9:1 hexanes/ethyl acetate). 1 H NMR (500

- MHz, CDCl₃) δ : 8.15 (d, J = 8.0 Hz, 1H) 7.56 (d, J = 8.0 Hz, 1H), 7.35 (t, J = 7.7 Hz, 1H), 7.24 (m, 2H), 3.81 (s, 3H), 3.49 (s, 3H), 2.70 (d, J = 13.4 Hz, 1H), 2.48 (d, J = 13.4 Hz, 1H), 2.06 (m, 3H), 2.00-1.94 (m, 3H), 1.77-1.66 (m, 9H), 1.62 (s, 9H); 13 C{ 1 H} NMR (126 MHz, CDCl₃) δ : 170.8, 169.9, 149.3, 135.9, 127.6, 125.1, 123.3, 122.3, 119.9, 117.0, 115.5, 106.7, 96.7, 84.2, 53.7, 52.0, 39.1, 37.4, 36.7, 31.4, 28.5, 28.3; IR (film) v/cm⁻¹ 3447 (w), 2922 (s), 2852 (m), 1735 (s), 1559 (w), 1453 (m), 1373 (m), 1240 (m), 1156 (m), 1097 (m), 892 (w), 748 (w); HRMS (APCI) m/z: [M + H]+ calc. for C₃₀H₃₈N₃O₆+, 536.2755, found 536.2744; mp: 104-105 °C.
- (4g) 5-(tert-butyl) 3-methyl (3R,5R)-3-((3R,5R,7R)-adamantan-1-yl)-5-phenyl-4,5-dihydro-3H-pyrazole-3,5-dicarboxylate. (343 mg, 95% yield). Colorless solid. $R_f = 0.27$ (49:1 hexanes/ethyl acetate). ¹H NMR (600 MHz, C_6C_6) δ: 7.49-7.46 (m, 2H), 7.06-7.02 (m, 2H), 6.97-6.94 (m, 1H), 2.99 (s, 3H), 2.91 (d, J = 13.4 Hz, 1H), 2.63 (d, J = 13.4 Hz, 1H), 2.24-2.19 (m, 3H), 1.89 (m, 3H), 1.71-1.66 (m, 3H), 1.55 (m, 6H), 1.30 (s, 9H); $^{13}C_6^{11}$ H} NMR (126 MHz, CDCl₃) δ: 171.0, 169.1, 138.3, 128.5, 128.0, 126.1, 105.7, 101.2, 83.1, 51.9, 38.9, 37.4, 36.8, 32.4, 28.5, 28.0; IR (powder) v/cm^{-1} 3059 (w), 2906 (s), 2852 (m), 1730 (s), 1599 (w), 1561 (w), 1449 (m), 1368 (m), 1240 (m), 1157 (m), 1116 (m), 1029 (w), 748 (w), 697 (w); HRMS (APCI) m/z: [M + H]+ calc. for $C_{26}H_{35}N_2O_4+$, 439.2591, found 439.2575; mp: 105-106 °C.
- **(4h)** 5-(1-(tert-butoxycarbonyl)piperidin-4-yl) 3-methyl (3R,5R)-3-((3R,5R,7R)-adamantan-1-yl)-5-phenyl-4,5dihydro-3H-pyrazole-3,5-dicarboxylate. (1.31 g, 58% yield). Colorless solid. $R_f = 0.29$ (4:1 hexanes/ethyl acetate). ¹H NMR $(500 \text{ MHz}, \text{CDCl}_3) \delta: 7.32-7.24 \text{ (m, 5H)}, 5.05 \text{ (sep, J} = 3.5 \text{ Hz},$ 1H), 3.51-3.43 (m, 1H), 3.37 (s, 3H), 3.36-3.32 (m, 1H), 3.30 (m, 2H), 2.60 (d, J = 13.8 Hz, 1H), 2.46 (d, J = 13.8 Hz, 1H),2.05 (s, 3H), 1.98-1.91 (m, 3H), 1.84-1.78 (m, 1H), 1.76-1.61 (m, 9H), 1.54-1.50 (m, 3H), 1.43 (s, 9H); ¹³C{¹H} NMR (126 MHz, CDCl₃) δ: 170.8, 169.4, 154.8, 137.9, 128.7, 128.3, 126.0, 105.9, 100.6, 79.8, 71.6, 52.0, 38.9, 37.3, 36.7, 32.3, 30.3, 30.2, 28.5, 28.4; IR (powder) $v/cm^{-1} 3013$ (w), 2925 (w), 2908 (w), 2851 (m), 1752 (m), 1727 (s), 1694 (s), 1557 (w), 1497 (w), 1399 (m), 1249 (s), 1165 (s), 1083 (m), 1033 (m), 759 (m), 705 (m); HRMS (APCI) m/z: [M + H]+ calc. for C₃₂H₄₄N₃O₆+, 566.3225, found 566.3226; mp: 114-116 °C.
- 3-methyl 5-phenyl (3R,5R)-3-((3R,5R,7R)adamantan-1-yl)-5-phenyl-4,5-dihydro-3H-pyrazole-3,5dicarboxylate. (322 mg, 83% yield). Colorless solid. $R_f = 0.17$ (9:1 hexanes/ethyl acetate). ¹H NMR (600 MHz, CDCl₃) δ: 7.38-7.33 (m, 6H), 7.32-7.29 (m, 1H), 7.25-7.21 (m, 1H), 7.06-7.03 (m, 2H), 3.43 (s, 3H), 2.74 (d, J = 13.8 Hz, 1H), 2.54 (d, J = 13.8 Hz, 1H), 2.06 (s, 3H), 2.02-1.97 (m, 3H), 1.76-1.66 (m, 6H), 1.60-1.56 (m, 3H); ${}^{13}C\{{}^{1}H\}$ NMR (126 MHz, CDCl₃) δ: 170.6, 168.7, 150.7, 137.4, 129.5, 128.8, 126.3, 125.9, 121.2, 106.2, 100.6, 51.9, 38.9, 37.2, 36.9, 32.4, 28.3; IR (powder) v/cm⁻¹ 3069 (w), 3016 (w), 2914 (w), 2853 (w), 1775 (m), 1723 (m), 1592 (w), 1558 (w), 1494 (w), 1239 (m), 1184 (s), 1071 (m), 755 (m), 739 (m), 698 (m), 689 (m); HRMS (APCI) m/z: [M + H]+ calc. for $C_{28}H_{31}N_2O_4$ +, 459.2278, found 459.2273; mp: 109-110 °C.
- (4j) 5-(4-benzoylphenyl) 3-methyl (3R,5R)-3-((3R,5R,7R)-adamantan-1-yl)-5-phenyl-4,5-dihydro-3H-pyrazole-3,5-dicarboxylate. (350 mg, 95% yield). Colorless solid. $R_f = 0.11$ (9:1 hexanes/ethyl acetate). ¹H NMR (500 MHz, CDCl₃) δ: 7.84 (m, 2H), 7.78 (m, 2H), 7.59 (m, 1H), 7.48 (m, 1H), 7.38

(d, J=4.4 Hz, 4H), 7.35 (m, 1H), 7.19 (m, 2H), 3.42 (s, 3H), 2.75 (d, J=13.8 Hz, 1H), 2.57 (d, J=13.8 Hz, 1H), 2.07 (m, 3H), 2.03-1.97 (m, 3H), 1.7-1.67 (m, 6H), 1.60 (m, 3H); 13 C{ 1 H} NMR (126 MHz, CDCl₃) δ : 195.6, 170.6, 168.4, 153.9, 137.5, 137.3, 135.7, 132.7, 131.8, 130.1, 129.0, 128.8, 128.5, 126.0, 121.3, 106.4, 100.7, 52.1, 39.1, 37.4, 36.7, 32.5, 28.5; IR (film) ν/cm^{-1} 3060 (w), 2907 (m), 2852 (m), 1753 (m), 1733 (m), 1661 (m), 1599 (m), 1582 (w), 1499 (w), 1447 (m), 1277 (m), 1230 (m), 1196 (s), 1164 (m), 1088 (m), 734 (w), 701 (m); HRMS (APCI) m/z: [M + H]+ calc. for $C_{35}H_{35}N_2O_5+$, 563.2541, found 563.2528; mp: 102-109 °C.

(4k) 5-((1R,2S,5R)-2-isopropyl-5-methylcyclohexyl) 3methyl (3R,5R)-3-((3R,5R,7R)-adamantan-1-yl)-5-phenyl-4,5dihydro-3H-pyrazole-3,5-dicarboxylate. (380 mg, 39% yield). Colorless solid. R_f = 0.38 (9:1 hexanes/ethyl acetate). ¹H NMR (500 MHz, CDCl₃) δ: 7.32-7.26 (m, 3H), 7.26-7.23 (m, 2H), 4.77 (dt, J = 4.4, 10.9 Hz, 1H), 3.44 (s, 3H), 2.61 (d, J = 13.9Hz, 1H), 2.41 (d, J = 13.9 Hz, 1H), 2.04 (m, 3H), 1.97-1.90(m, 4H), 1.80-1.61 (m, 10H), 1.54-1.50 (m, 3H), 1.49-1.38 (m, 2H), 1.06-0.91 (m, 2H), 0.88 (d, J = 6.5 Hz, 3H), 0.82 (d, J =7.0 Hz, 3H), 0.65 (d, J = 7.0 Hz, 3H); ${}^{13}C\{{}^{1}H\}$ NMR (126 MHz, CDCl₃) δ: 171.1, 169.8, 137.9, 128.6, 128.2, 125.9, 106.1, 101.2, 76.7, 52.0, 46.9, 40.3, 39.0, 37.3, 36.7, 34.2, 32.2, 31.5, 28.5, 26.1, 23.3, 22.1, 20.8, 16.1; IR (powder) v/cm^{-1} 3066 (w), 2954 (w), 2921 (m), 2921 (m), 2851 (m), 1726 (m), 1599 (w), 1572 (w), 1448 (w), 1424 (w), 1250 (s), 1117 (m), 1100 (m), 1031 (w), 726 (m), 694 (m); HRMS (APCI) m/z: [M + H]+ calc. for C₃₂H₄₅N₂O₄+, 521.3374. found 521.3366; mp: 124-128 °C.

General Procedures for the Photodenitrogenation Reactions (Notes: The 450W Hg lamp produces significant heat; fans are installed to help circulate warm air out of the box containing the irradiation setup. The sample should be crushed into a very thin layer to ensure adequate light penetration. Identical suspension preparations can be done for pyrazoline derivatives 4c and 4i to afford the corresponding cyclopropanes with similar stereoselectivities as their bulk powder irradiations. It is imperative that the aqueous solution is stirring consistently during preparation to achieve high-quality suspensions; irregularities were observed to result in significant aggregation of reprecipitated sample. The chosen stirbar should be approximately equal in length to the diameter of the reaction vessel and stirred at a rate such that there is a visible vortex. The substrate should be added dropwise to aqueous solution on the sides of the vortexing solution (rather than directly in the center) to ensure the sample is equally dispersed.)

Solution-phase irradiations: Pyrazolines **4a–k** (2.0 mg) were each dissolved in 0.5 mL C₆D₆ in NMR tubes and sparged with Argon for 20 min through an appropriately-sized septum. The NMR tubes were capped and sealed with Parafilm, then irradiated in the Hanovia photochemical reactor and monitored by ¹H NMR at 2.5 min intervals. Reactions were irradiated to 100% conversion of starting material, typically 10-25 min; purification was not attempted with these samples.

Bulk-solid irradiations: Solid pyrazolines **4a–k** (2.0 mg) were each crushed between microscope slides for about 5 seconds until a translucent sample was obtained. Samples were then irradiated in the Hanovia photochemical reactor for times identical to their solution-phase counterparts. The slides were then washed with CH₂Cl₂ or CDCl₃ and concentrated under

rotary evaporation; purification was not attempted with these samples.

Aqueous suspension irradiations of pyrazoline 4h: 4h (200.0 mg, 0.35 mmol) was dissolved in 5.0 mL of acetonitrile and added dropwise to a rapidly stirring aqueous solution of cetrimonium bromide (CTAB) (100 mL, 5% CMC of CTAB) in a Pyrex container that was pre-treated with Sigmacote (note 4). The resulting cloudy suspension was sonicated for 5 min, then irradiated in Hanovia photochemical reactor for 2 h. The reaction was briefly sonicated every 30 min to minimize any material buildup on the walls of the reaction vessel. Upon completion, the organics were extracted with EtOAc (3 x 25.0 mL), washed with brine (1 x 15 mL), dried over Na₂SO₄, then concentrated directly onto silica gel (2.5 g). Purification via column chromatography (30 g silica gel, 400 mL 12.5:1 hexanes/ethyl acetate \rightarrow 200 mL 9:1 hexanes/ethyl acetate \rightarrow 200 mL 6.7:1 hexanes/ethyl acetate) afforded 5h as a colorless solid (103 mg, 54% yield).

Characterization Data for Cyclopropanes 5a-k

- (5a) Dimethyl (1S,2S)-1-((3S,5S,7S)-adamantan-1-yl)-2-phenylcyclopropane-1,2-dicarboxylate. Colorless solid. $R_f=0.38$ (9:1 hexanes/ethyl acetate). 1H NMR (600 MHz, CDCl₃) δ : 7.49-7.46 (m, 2H), 7.26-7.19 (m, 3H), 3.66 (s, 3H), 3.13 (s, 3H), 2.01-1.97 (m, 3H), 1.99 (d, J=6.2 Hz, 1H), 1.95 (d, J=6.2 Hz, 1H), 1.73-1.61 (m, 9H); $^{13}C\{^1H\}$ NMR (126 MHz, CDCl₃) δ : 171.4, 170.5, 136.5, 131.0, 127.75, 127.74, 52.5, 51.3, 48.2, 39.4, 38.5, 36.9, 34.5, 28.9, 15.2; IR (powder) v/cm^{-1} 3055 (w), 2913 (m), 2850 (m), 1723 (s), 1597 (w), 1446 (m), 1431 (m), 1224 (s), 1206 (s), 1151 (m), 1068 (m), 741 (m), 705 (s); HRMS (APCI) m/z: [M + H]+ calc. for $C_{23}H_{29}O_4+$, 369.2060, found 369.2058; mp: 111-113 $^{\circ}C$.
- (**5b**) Dimethyl (1S,2S)-1-((3S,5S,7S)-adamantan-1-yl)-2-(4-(trifluoromethyl)phenyl)cyclopropane-1,2-dicarboxylate. Colorless solid. $R_f = 0.69$ (9:1 hexanes/ethyl acetate). ¹H NMR (500 MHz, CDCl₃) δ: 7.61 (d, J = 8.3 Hz, 2H), 7.51 (d, J = 8.3 Hz, 2H), 3.67 (s, 3H), 3.15 (s, 3H), 2.03 (d, J = 6.3 Hz, 1H), 2.02-1.97 (m, 3H), 2.01 (d, J = 6.3 Hz, 1H), 1.90-1.85 (m, 3H), 1.73-1.67 (m, 6H), 1.66-1.61 (m, 3H); ¹³C {¹H} NMR (126 MHz, CDCl₃) δ: 170.7, 170.2, 140.6, 131.4, 130.3 (q, J = 32.5 Hz), 127.4 (q, J = 272.3 Hz), 124.7 (q, J = 3.7 Hz), 52.7, 51.4, 48.6, 39.4, 38.2, 36.9, 34.6, 29.9, 15.4; IR (powder) ν/cm⁻¹ 3013 (w), 2905 (m), 2849 (m), 1725 (s), 1614 (w), 1445 (w), 1430 (w), 1323 (m), 1238 (m), 1160 (m), 1108 (s), 1060 (s), 840 (m), 791 (w), 725 (m); HRMS (APCI) m/z: [M + H]+ calc. for C₂₄H₂₈F₃O₄+, 437.1934, found 437.1940; mp: 183-184 °C.
- (5c) Dimethyl (1S,2S)-1-((3S,5S,7S)-adamantan-1-yl)-2-(4-bromophenyl)cyclopropane-1,2-dicarboxylate. (30 mg, 71% yield). Colorless solid. $R_f=0.69$ (9:1 hexanes/ethyl acetate). ¹H NMR (500 MHz, CDCl₃) δ: 7.38 (m, 4H), 3.66 (s, 3H), 3.20 (s, 3H), 2.01-1.97 (m, 3H), 1.98 (d, J=6.2 Hz, 1H), 1.94 (d, J=6.2 Hz, 1H), 1.88-1.83 (m, 3H), 1.72-1.66 (m, 6H), 1.65-1.60 (m, 3H); ¹³C { ¹H } NMR (126 MHz, CDCl₃) δ: 171.0, 170.4, 135.6, 132.7, 130.9, 122.1, 52.6, 51.5, 48.5, 39.5, 37.8, 36.9, 34.6, 28.8, 15.4; IR (powder) ν /cm⁻¹ 3014 (w), 2913 (m), 2849 (m), 1726 (s), 1716 (s), 1487 (m), 1450 (m), 1483 (m), 1235 (s), 1193 (m), 1175 (m), 1065 (s), 851 (w), 779 (w), 711 (m); HRMS (APCI) m/z: [M+H]+ calc. for $C_{23}H_{28}BrO_4+$, 447.1166, found 447.1154; mp: 188-189 °C.
- **(5d)** *Dimethyl* (1S,2S)-1-((3S,5S,7S)-adamantan-1-yl)-2-(4-methoxyphenyl)cyclopropane-1,2-dicarboxylate. Colorless

- solid. $R_f = 0.28$ (9:1 hexanes/ethyl acetate). ¹H NMR (500 MHz, CDCl₃) δ : 7.40 (m, 2H), 6.78 (m, 2H), 3.76 (s, 3H), 3.65 (s, 3H), 3.19 (s, 3H), 1.98 (m, 3H), 1.92 (s, 2H), 1.72-1.60 (m, 9H); ¹³C {¹H} NMR (126 MHz, CDCl₃) δ : 171.6, 170.7, 159.1, 132.1, 128.4, 113.1, 55.3, 52.4, 51.3, 48.3, 39.5, 37.7, 36.9, 34.5, 28.9, 15.3; IR (powder) v/cm⁻¹ 3027 (w), 2909 (m), 2846 (m), 1718 (s), 1683 (w), 1611 (m), 1580 (w), 1513 (s), 1430 (m), 1228 (s), 1193 (m), 1176 (s), 1066 (s), 1032 (m), 831 (m), 799 (m), 734 (w); HRMS (APCI) m/z: [M + H]+ calc. for $C_{24}H_{31}O_5+$, 399.2166, found 399.2170; mp: 134-135 °C.
- (5e) Dimethyl (1S,2S)-1-((3S,5S,7S)-adamantan-1-yl)-2-(naphthalen-1-yl)cyclopropane-1,2-dicarboxylate. Colorless solid. $R_f = 0.36$ (9:1 hexanes/ethyl acetate). ¹H NMR (500 MHz, CDCl₃) δ : 8.83 (d, J = 8.4 Hz, 1H), 8.40 (d, J = 8.4 Hz, 1.6H), 7.82 (m, 3.4H), 7.76 (m, 3.8H), 7.53 (m, 3.8H), 7.46 (m, 3H), 7.39 (m, 3H), 3.61 (s, 4.8H), 3.58 (s, 3H), 3.17 (s, 4.8H), 2.70 (s, 3H), 2.38 (d, J = 5.8 Hz, 1.6H), 2.17 (d, J = 5.4Hz, 1H), 2.11 (m, 3H), 2.08-1.97 (m, 17H), 1.95-1.90 (m, 3.6H), 1.87-1.79 (m, 6H), 1.77-1.65 (m, 17H); ¹³C{¹H} NMR (126 MHz, CDCl₃) δ: 171.5, 171.1, 170.9, 170.7, 134.1, 134.0, 133.9, 133.2, 132.4, 130.9, 129.2, 129.1, 128.9, 128.6, 128.5, 127.8, 126.2, 125.8, 125.5, 125.3, 124.9, 124.87, 124.6, 52.6, 52.55, 51.4, 50.8, 47.6, 47.4, 39.6, 39.3, 38.5, 37.3, 37.0, 36.9, 35.0, 34.97, 29.0, 28.9, 18.2, 17.5 (one -1-naphthyl peak unaccounted for); IR (powder) v/cm⁻¹ 3046 (w), 3002 (w), 2908 (m), 2886 (m), 2848 (m), 1718 (s), 1595 (w), 1508 (w), 1430 (m), 1397 (w), 1323 (w), 1221 (s), 1194 (m), 1075 (m), 950 (m), 876 (m), 797 (m), 790 (m), 773 (s), 731 (m); HRMS (APCI) m/z: [M + H]+ calc. for $C_{27}H_{31}O_4$ +, 419.2217, found 419.2214; mp: 187-196 °C. (Note: **5e** and **8e** were obtained as an inseparable mixture; the empirical spectra are reported.)
- (5f) Dimethyl (1S,2S)-1-((3S,5S,7S)-adamantan-1-yl)-2-(1-(tert-butoxycarbonyl)-1H-indol-3-yl)cyclopropane-1,2-dicarboxylate. Colorless solid. $R_f=0.39$ (9:1 hexanes/ethyl acetate). ¹H NMR (600 MHz, CDCl₃) δ: 8.06 (br. s, 1H), 7.96 (m, 1H), 7.46 (br s, 1H), 7.28-7.22 (m, 3H), 3.64 (s, 3H), 3.06 (s, 3H), 2.09 (d, J=5.8 Hz, 1H), 2.02 (m, 3H), 1.97-1.92 (m, 3H), 1.89 (d, J=5.8 Hz, 1H), 1.74-1.69 (m, 6H), 1.67 (m, 3H), 1.64 (s, 9H); 13 C{ 1 H} NMR (126 MHz, CDCl₃) δ: 171.1, 171.0, 149.5, 135.6, 129.8, 126.7, 124.4, 122.4, 122.3, 117.7, 114.9, 83.9, 52.5, 51.2, 48.5, 39.8, 36.9, 34.3, 30.6, 28.9, 28.3, 16.5; IR (powder) ν/cm⁻¹ 3059 (w), 2910 (m), 2850 (m), 1727 (s), 1608 (w), 1566 (w), 1451 (m), 1432 (m), 1373 (s), 1222 (s), 1152 (s), 1104 (m), 1059 (s), 852 (w), 802 (w), 764 (m), 746 (m); HRMS (APCI) m/z: [M + H]+ calc. for C₃₀H₃₈NO₆+, 508.2694, found 508.2698; mp: 59-63 °C.
- (5g) 2-(tert-butyl) 1-methyl (1S,2S)-1-((3S,5S,7S)-adamantan-1-yl)-2-phenylcyclopropane-1,2-dicarboxylate. Colorless solid. $R_f = 0.50$ (9:1 hexanes/ethyl acetate). ¹H NMR (600 MHz, CDCl₃) δ : 7.47-7.43 (m, 2H), 7.23-7.16 (m, 3H), 3.12 (s, 3H), 2.02-1.94 (m, 6H), 1.90 (d, J = 6.0 Hz, 1H), 1.87 (d, J = 6.0 Hz, 1H), 1.79-1.75 (m, 3H), 1.72-1.64 (m, 6H), 1.38 (s, 9H); ¹³C{¹H} NMR (126 MHz, CDCl₃) δ : 170.8, 169.9, 137.2, 131.0, 127.5, 127.4, 81.8, 51.2, 48.2, 40.5, 39.4, 37.0, 34.8, 28.9, 27.9, 14.9; IR (powder) v/cm^{-1} 3050 (w), 2915 (m), 2850 (m), 1727 (m), 1714 (s), 1599 (w), 1447 (m), 1364 (m), 1237 (s), 1159 (s), 1062 (m), 730 (m), 699 (m); HRMS (APCI) m/z: [M + H]+ calc. for $C_{26}H_{35}O_4+$, 411.2530, found 411.2518; mp: 100-102 °C.
- **(5h)** 2-(1-(tert-butoxycarbonyl)piperidin-4-yl) 1-methyl (1S,2S)-1-((3S,5S,7S)-adamantan-1-yl)-2-

- phenylcyclopropane-1,2-dicarboxylate. (103 mg, 54% yield). Colorless solid. R_f = 0.24 (9:1 hexanes/ethyl acetate). 1 H NMR (500 MHz, CDCl₃) δ: 7.49-7.42 (m, 2H), 7.25-7.17 (m, 3H), 4.91 (sep, , J = 3.7 Hz, 1H), 3.67-3.59 (m, 1H), 3.41-3.35 (m, 1H), 3.34-3.28 (m, 1H), 3.23-3.16 (m, 1H), 3.16 (s, 3H), 1.99 (m, 3H), 1.97 (d, J = 6.2 Hz, 1H), 1.95 (d, J = 6.2 Hz, 1H), 1.95-1.90 (m, 3H), 1.88-1.81 (m, 1H), 1.76-1.60 (m, 12H), 1.45 (s, 9H); 13 C 1 H 1 NMR (126 MHz, CDCl₃) δ: 170.5, 170.3, 154.8, 136.7, 131.0, 127.8, 127.7, 79.8, 70.9, 51.3, 48.4, 39.5, 39.2, 36.9, 34.7, 30.6, 30.1, 28.8, 28.6, 15.3; IR (film) ν /cm $^{-1}$ 3025 (w), 2911 (m), 2852 (m), 1734 (s), 1718 (s), 1683 (s), 1602 (w), 1478 (w), 1425 (s), 1222 (s), 1197 (s), 1157 (s), 864 (m), 757(w), 698 (s); HRMS (APCI) m/z: [M + H]+ calc. for C₃₂H₄₄NO₆+, 538.3163, found 538.3167; mp: 139-142 °C.
- (5j) 2-(4-benzoylphenyl) 1-methyl (1S,2S)-1-((3S,5S,7S)-adamantan-1-yl)-2-phenylcyclopropane-1,2-dicarboxylate. Colorless solid. R_f = 0.20 (9:1 hexanes/ethyl acetate). ¹H NMR (500 MHz, CDCl₃) δ : 7.82 (m, 2H), 7.77 (m, 2H), 7.57 (m, 3H), 7.47 (m, 2H), 7.33-7.24 (m, 3H), 7.12 (m, 2H), 3.19 (s, 3H), 2.12 (s, 2H), 2.07-2.01 (m, 6H), 1.87-1.81 (m, 3H), 1.76-1.65 (m, 6H); 13 C (1 H} NMR (126 MHz, CDCl₃) δ : 195.6, 170.2, 169.1, 154.1, 137.6, 135.8, 135.3, 132.6, 131.8, 131.2, 130.1, 128.5, 128.2, 128. 0, 121.2, 51.4, 49.0, 39.7, 38.9, 36.9, 34.9, 28.9, 15.6; IR (film) ν /cm⁻¹ 3090 (w), 3058 (w), 2927 (w), 2857 (w), 1735 (w), 11692 (m), 1632 (w), 1596 (w), 1493 (m), 1447 (m), 1373 (w), 1186 (w), 1090 (m), 852 (w), 742 (m), 702 (s), 634 (m); HRMS (APCI) m/z: [M + H]+ calc. for $C_{35}H_{35}O_5+$, 535.2479, found 535.2469; mp: 125-127 °C.
- (5k) 2-((1R,2S,5R)-2-isopropyl-5-methylcyclohexyl) 1-(1S,2S)-1-((3S,5S,7S)-adamantan-1-yl)-2phenylcyclopropane-1,2-dicarboxylate. Colorless solid. $R_f =$ 0.58 (9:1 hexanes/ethyl acetate). ¹H NMR (500 MHz, CDCl₃) δ : 7.44-7.42 (m, 2H), 7.23-7.16 (m, 3H), 4.58 (dt, J = 4.3, 10.8 Hz, 1H), 3.15 (s, 3H), 2.01-1.93 (m, 6H), 1.95 (d, J = 6.1 Hz, 1H), 1.92 (d, J = 6.1 Hz, 1H), 1.85-1.79 (m, 1H), 1.78-1.72(m, 4H), 1.71-1.64 (m, 6H), 1.65-1.58 (m, 3H), 1.44-1.31 (m, 2H), 1.02-0.92 (m, 1H), 0.82 (d, J = 6.6 Hz, 3H), 0.79 (d, J =7.0 Hz, 3H), 0.75 (m, 1H), 0.54 (d, J = 7.0 Hz, 3H); ${}^{13}C\{{}^{1}H\}$ NMR (126 MHz, CDCl₃) δ: 170.8, 170.6, 137.1, 130.9, 127.5, 75.9, 51.2, 48.5, 47.1, 40.1, 39.5, 39.1, 36.9, 34.4, 34.3, 31.4, 28.9, 26.0, 23.3, 22.1, 20.9, 16.0, 15.3; IR (powder) v/cm⁻¹ 3055 (w), 2953 (m), 2910 (s), 2851 (m), 1724 (s), 1600 (w), 1492 (w), 1447 (m), 1249 (s), 1199 (m), 1177 (s), 1100 (m), 733 (m), 701 (s), 516 (m); HRMS (APCI) m/z: [M + H]+ calc. for C₃₂H₄₅O₄+, 493.3312, found 493.3323; mp: 150-154 °C.

General Procedures for the Thermal Denitrogenation Reactions

Solution-phase thermal denitrogenation: Pyrazoline **4h** (15.0 mg, 0.027 mmol) was dissolved in a minimal amount of toluene and added to 5 mL of refluxing toluene. After 90 sec, the reaction was cooled to room temperature and concentrated under rotary evaporation. Spectral data for **5h** match those from the solution photochemical denitrogenation reactions.

Bulk-solid thermal denitrogenation: Solid pyrazoline **4h** (15.0 mg, 0.027 mmol) was ground into a translucent powder and heated at 110 °C in a 1 DRAM vial for 90 sec. Spectral data for **5h** match those from the solid-state photochemical denitrogenation reactions.

ASSOCIATED CONTENT

Supporting Information

The Supporting Information is available free of charge on the ACS Publications website.

Spectroscopic ¹H and ¹³C{¹H} characterization data for **6**, **7a–k**, **4a–k**, **5a–k**, **9**, **10**, **11b**, **11c**, **11e–k**; single-crystal X-ray thermal ellipsoid plots and select crystallography data for compounds **4a**, **5a**, **4g**, **4i**, **4k**, **5k**; DSC curves for compounds **4h**, **5h**, **4k**, **5k**; TGA curve for **4h** (PDF).

Single-crystal X-ray structure for compound **4a** (CIF) Single-crystal X-ray structure for compound **5a** (CIF) Single-crystal X-ray structure for compound **4g** (CIF) Single-crystal X-ray structure for compound **4i** (CIF) Single-crystal X-ray structure for compound **4k** (CIF) Single-crystal X-ray structure for compound **5k** (CIF)

Pyrazoline **4k** heated at 110 $^{\circ}$ C and monitored using an optical microscope equipped with a camera; N₂ can be seen escaping a well-maintained crystal (AVI).

AUTHOR INFORMATION

Corresponding Author

*mgg@chem.ucla.edu

Notes

The authors declare no competing financial interests.

ACKNOWLEDGMENT

The authors thank the National Science Foundation (CHE-1855342 for M.G.G.; NSF-OAC-1940307 for S.A.L.) for financial support. D.A. and S.A.L. appreciate the assistance from the Northeastern Research Computing Team and access to the computing resources of the Discovery cluster. The authors thank Dr. Saeed Khan (UCLA) for X-ray analysis.

REFERENCES

- Ebner, C.; Carreira, E. M. Cyclopropanation Strategies in Recent Total Syntheses. *Chem. Rev.* 2017, 117, 11651–11679.
- (2) Dian, L.; Marek, I. Asymmetric Preparation of Polysubstituted Cyclopropanes Based on Direct Functionalization of Achiral Three-Membered Carbocycles. Chem. Rev. 2018, 118, 8415– 8434
- (3) Chawner, S. J.; Cases-Thomas, M. J.; Bull, J. A. Divergent Synthesis of Cyclopropane-Containing Lead-Like Compounds, Fragments and Building Blocks through a Cobalt Catalyzed

- Cyclopropanation of Phenyl Vinyl Sulfide. European J. Org. Chem. 2017, 2017, 5015–5024.
- (4) Wu, W.; Lin, Z.; Jiang, H. Recent Advances in the Synthesis of Cyclopropanes. Org. Biomol. Chem. 2018, 16, 7315–7329.
- (5) Jiang, H.; Fu, W.; Chen, H. Palladium-Catalyzed Cross-Coupling Reactions of Electron-Deficient Alkenes with N-Tosylhydrazones: Functional-Group-Controlled C-C Bond Construction. Chem. A Eur. J. 2012, 18, 11884–11888.
- (6) Chen, H.; Zhang, L. A Desulfonylative Approach in Oxidative Gold Catalysis: Regiospecific Access to Donor-Substituted Acyl Gold Carbenes. Angew. Chemie - Int. Ed. 2015, 54, 11775– 11779
- (7) Deng, C.; Liu, H. K.; Zheng, Z. B.; Wang, L.; Yu, X.; Zhang, W.; Tang, Y. Copper-Catalyzed Enantioselective Cyclopropanation of Internal Olefins with Diazomalonates. *Org. Lett.* 2017, 19, 5717–5719.
- (8) Antoniak, D.; Barbasiewicz, M. Corey-Chaykovsky Cyclopropanation of Nitronaphthalenes: Access to Benzonorcaradienes and Related Systems. Org. Lett. 2019, 21, 9320–9325
- (9) Marsini, M. A.; Reeves, J. T.; Desrosiers, J. N.; Herbage, M. A.; Savoie, J.; Li, Z.; Fandrick, K. R.; Sader, C. A.; McKibben, B.; Gao, D. A.; Cui, J.; Gonnella, N. C.; Lee, H.; Wei, X.; Roschangar, F.; Lu, B. Z.; Senanayake, C. H. Diastereoselective Synthesis of α-Quaternary Aziridine-2-Carboxylates via Aza-Corey-Chaykovsky Aziridination of N-Tert-Butanesulfinyl Ketimino Esters. *Org. Lett.* 2015, 17, 5614–5617.
- (10) Bos, M.; Huang, W. S.; Poisson, T.; Pannecoucke, X.; Charette, A. B.; Jubault, P. Catalytic Enantioselective Synthesis of Highly Functionalized Difluoromethylated Cyclopropanes. *Angew. Chemie - Int. Ed.* 2017, 56, 13319–13323.
- (11) Nam, D.; Steck, V.; Potenzino, R. J.; Fasan, R. A Diverse Library of Chiral Cyclopropane Scaffolds via Chemoenzymatic Assembly and Diversification of Cyclopropyl Ketones. *J. Am. Chem. Soc.* 2021, 143, 2221–2231.
- (12) Gao, L.; Hwang, G. S.; Ryu, D. H. Oxazaborolidinium Ion-Catalyzed Cyclopropanation of α-Substituted Acroleins: Enantioselective Synthesis of Cyclopropanes Bearing Two Chiral Quaternary Centers. J. Am. Chem. Soc. 2011, 133, 20708–20711.
- (13) Cohen, Y.; Augustin, A. U.; Levy, L.; Jones, P. G.; Werz, D. B.; Marek, I. Regio- and Diastereoselective Copper-Catalyzed Carbomagnesiation for the Synthesis of Penta- and Hexa-Substituted Cyclopropanes. *Angew. Chemie - Int. Ed.* 2021, 60, 11804–11808.
- (14) Müller, D. S.; Marek, I. Copper Mediated Carbometalation Reactions. Chem. Soc. Rev. 2016, 45, 4552–4566. https://doi.org/10.1039/c5cs00897b.
- Borovika, A.; Albrecht, J.; Li, J.; Wells, A. S.; Briddell, C.;
 Dillon, B. R.; Diorazio, L. J.; Gage, J. R.; Gallou, F.; Koenig, S.
 G.; Kopach, M. E.; Leahy, D. K.; Martinez, I.; Olbrich, M.;
 Piper, J. L.; Roschangar, F.; Sherer, E. C.; Eastgate, M. D. The
 PMI Predictor App to Enable Green-by-Design Chemical
 Synthesis. Nat. Sustain. 2019, 2, 1034–1040.
- (16) Rinehart, K. L.; Van Auken, T. V. Light-Induced Decomposition of Pyrazolines. An Improved Entry into the Cyclopropane Series. *J. Am. Chem. Soc.* **1960**, *82*, 5251.
- (17) Van Auken, T. V.; Rinehart, K. L. Stereochemistry of the Formation and Decomposition of 1-Pyrazolines. *J. Am. Chem. Soc.* **1962**, *84*, 3736–3743.
- (18) Engel, P. S. Mechanism of the Thermal and Photochemical Decomposition of Azoalkanes. *Chem. Rev.* **1980**, *80*, 99–150.
- (19) Xu, W.; Wu, S.; Zhou, L.; Liang, G. Total Syntheses of Echinopines. Org. Lett. 2013, 15, 1978–1981.
- (20) Ramamurthy, V.; Sivaguru, J. Supramolecular Photochemistry as a Potential Synthetic Tool: Photocycloaddition. *Chem. Rev.* 2016, 116, 9914–9993.
- (21) Shiraki, S.; Vogelsberg, C. S.; Garcia-Garibay, M. A. Solid-State Photochemistry of Crystalline Pyrazolines: Reliable Generation and Reactivity Control of 1,3-Biradicals and Their Potential for the Green Chemistry Synthesis of Substituted Cyclopropanes. *Photochem. Photobiol. Sci.* 2012, 11, 1929–1937.
- (22) Allred, E. L.; Smith, R. L. Thermal and Photodecomposition Studies with the Exo- and Endo-5-Methoxy-2,3-Diazabicyclo

- [2.2.1] Hept-2-Ene System. J. Am. Chem. Soc. 1969, 91, 6766–6775.
- (23) Adam, W.; García, H.; Martí, V.; Moorthy, J. N.; Peters, K.; Peters, E. M. Photochemical Denitrogenation of Norbornene-Annelated 2,3- Diazabicyclo[2.1.1]Hept-2-Ene-Type Azoalkanes: Crystal-Lattice versus Zeolite-Interior Effects [8]. *J. Am. Chem. Soc.* **2000**, *122*, 3536–3537.
- (24) For more discussion on the synthesis of vicinal quaternary stereocenters, also see reference 25. Kohmoto, S.; Yamada, K.; Joshi, U.; Kawatuji, T.; Yamamoto, M.; Yamada, K. Photochemical Generation of 1,4-Diphenylbutane-1,4-Diyl. *J. Chem. Soc. Chem. Commun.* **1990**, No. 2, 127–129.
- (25) Peterson, E. A.; Overman, L. E. Contiguous Stereogenic Quaternary Carbons: A Daunting Challenge in Natural Products Synthesis. Proc. Natl. Acad. Sci. U. S. A. 2004, 101, 11943– 11948.
- (26) Long, R.; Huang, J.; Gong, J.; Yang, Z. Direct Construction of Vicinal All-Carbon Quaternary Stereocenters in Natural Product Synthesis. Nat. Prod. Rep. 2015, 32, 1584–1601.
- (27) Lovering, F.; Bikker, J.; Humblet, C. Escape from Flatland: Increasing Saturation as an Approach to Improving Clinical Success. J. Med. Chem. 2009, 52, 6752–6756.
- (28) Talele, T. T. The "Cyclopropyl Fragment" Is a Versatile Player That Frequently Appears in Preclinical/Clinical Drug Molecules. J. Med. Chem. 2016, 59, 8712–8756.
- (29) Bauer, M. R.; Fruscia, P. Di; Lucas, S. C. C.; Michaelides, I. N.; Nelson, J. E.; Storer, R. I.; Whitehurst, B. C. Put a Ring on It: Application of Small Aliphatic Rings in Medicinal Chemistry. RSC Med. Chem. 2021, 12, 448–471.
- (30) Ohno, M.; Itoh, M.; Umeda, M.; Furuta, R.; Kondo, K.; Eguchi, S. Conjugatively Stabilized Bridgehead Olefins: Formation and Reaction of Remarkably Stable Homoadamant-3-Enes Substituted with Phenyl and Methoxycarbonyl Groups. J. Am. Chem. Soc. 1996, 118, 7075–7082.
- (31) Adam, W.; Moorthy, J. N.; Nau, W. M.; Scaiano, J. C. Solvent Effect on Product Distribution in Photochemical Pathways of α C-N versus β C-C Cleavage of n,Π* Triplet-Excited Azoalkanes. J. Am. Chem. Soc. 1997, 119, 5550–5555.
- (32) Adam, W.; Nau, W. M.; Sendelbach, J.; Wirz, J. Identification of a Remarkably Long-Lived Azoalkane Triplet State. *J. Am. Chem. Soc.* **1993**, *115*, 12571–12572.
- (33) Kita, F.; Adam, W.; Jordan, P.; Nau, W. M.; Wirz, J. 1,3-Cyclopentanediyl Diradicals: Substituent and Temperature Dependence of Triplet-Singlet Intersystem Crossing. J. Am. Chem. Soc. 1999, 121, 9265–9275.
- (34) Abe, M.; Watanabe, S.; Tamura, H.; Boinapally, S.; Kanahara, K.; Fujiwara, Y. Substituent Effect on Reactivity of Triplet Excited State of 2,3- Diazabicyclo[2.2.1]Hept-2-Enes, DBH Derivatives: α C-N Bond Cleavage versus β C-C Bond Cleavage Manabu. J. Org. Chem. 2013, 78, 1940–1948.
- (35) While not focused on in this study, the minor diastereomers are also crystalline and should yield similar conclusions.
- (36) Attempts to shorten reaction times via elevated temperatures or the addition of Lewis acids resulted in messy product mixtures or diazoalkane coupling; the regioselectivities also suffered.
- (37) Dotson, J. J.; Garg, N. K.; Garcia-Garibay, M. A. Evaluation of the Photodecarbonylation of Crystalline Ketones for the Installation of Reverse Prenyl Groups on the Pyrrolidinoindoline Scaffold. *Tetrahedron* 2020, 131181.
- (38) Campos, L. M.; Dang, H.; Ng, D.; Yang, Z.; Martinez, H. L.; Garcia-Garibay, M. A. Engineering Reactions in Crystalline Solids: Predicting Photochemical Decarbonylation from Calculated Thermochemical Parameters. J. Org. Chem. 2002, 67, 3749–3754.
- (39) Dotson, J. J.; Liepuoniute, I.; Bachman, J. L.; Hipwell, V. M.; Khan, S. I.; Houk, K. N.; Garg, N. K.; Garcia-Garibay, M. A. Taming Radical Pairs in the Crystalline Solid State: Discovery and Total Synthesis of Psychotriadine. J. Am. Chem. Soc. 2021, 143, 4043–4054.
- (40) Gaussian 16, Revision C.01, M. J. Frisch, G. W. Trucks, H. B. Schlegel, G. E. Scuseria, M. A. Robb, J. R. Cheeseman, G. Scalmani, V. Barone, G. A. Petersson, H. Nakatsuji, X. Li, M. Caricato, A. V. Marenich, J. Bloino, B. G. Janesko, R. Gomperts, B. Mennucci, H. P. Hratchian, J. V. Ortiz, A. F. Izmaylov, J. L. Sonnenberg, D. Williams-Young, F. Ding, F.

- Lipparini, F. Egidi, J. Goings, B. Peng, A. Petrone, T. Henderson, D. Ranasinghe, V. G. Zakrzewski, J. Gao, N. Rega, G. Zheng, W. Liang, M. Hada, M. Ehara, K. Toyota, R. Fukuda, J. Hasegawa, M. Ishida, T. Nakajima, Y. Honda, O. Kitao, H. Nakai, T. Vreven, K. Throssell, J. A. Montgomery, Jr., J. E. Peralta, F. Ogliaro, M. J. Bearpark, J. J. Heyd, E. N. Brothers, K. N. Kudin, V. N. Staroverov, T. A. Keith, R. Kobayashi, J. Normand, K. Raghavachari, A. P. Rendell, J. C. Burant, S. S. Iyengar, J. Tomasi, M. Cossi, J. M. Millam, M. Klene, C. Adamo, R. Cammi, J. W. Ochterski, R. L. Martin, K. Morokuma, O. Farkas, J. B. Foresman, and D. J. Fox, Gaussian, Inc., Wallingford CT, 2016.
- (41) Zhao, Y.; Truhlar, D. G. The M06 Suite of Density Functionals for Main Group Thermochemistry, Thermochemical Kinetics, Noncovalent Interactions, Excited States, and Transition Elements: Two New Functionals and Systematic Testing of Four M06-Class Functionals and 12 Other Function. Theor. Chem. Acc. 2008, 120, 215–241.
- (42) Tomasi, J.; Mennucci, B.; Cammi, R. Quantum Mechanical Continuum Solvation Models. Chem. Rev. 2005, 105, 2999– 3093
- (43) Petersson, G. A.; Bennett, A.; Tensfeldt, T. G.; Al-Laham, M. A.; Shirley, W. A.; Mantzaris, J. A Complete Basis Set Model Chemistry. I. The Total Energies of Closed-Shell Atoms and Hydrides of the First-Row Elements. J. Chem. Phys. 1988, 89, 2193–2218.
- (44) Lopez, S. A.; Pourati, M.; Gais, H. J.; Houk, K. N. How Torsional Effects Cause Attack at Sterically Crowded Concave Faces of Bicyclic Alkenes. J. Org. Chem. 2014, 79, 8304–8312.
- (45) Lopez, S. A.; Munk, M. E.; Houk, K. N. Mechanisms and Transition States of 1,3-Dipolar Cycloadditions of Phenyl Azide with Enamines: A Computational Analysis. *J. Org. Chem.* 2013, 78, 1576–1582.
- (46) Chen, S.; Hu, T.; Houk, K. N. Energy of Concert and Origins of Regioselectivity for 1,3-Dipolar Cycloadditions of Diazomethane. J. Org. Chem. 2021, 86, 6840–6846.
- (47) Schmidt, G. M. . Photodimerization in the Solid State. Pure Appl. Chem 1971, 27, 647–678.
- (48) The conformations observed from the recrystallized product structures do not necessarily reflect those of the as-formed product in the reacting crystals.
- (49) Anslyn, E. A.; Dougherty, D. A. *Modern Physical Organic Chemistry*, University Science Books: Sausalito, CA, 2006.
- (50) Kreft, A.; Alexander, L.; Grunenberg, J.; Jones, P. G.; Werz, D. B. Kinetic Studies of Donor Acceptor Cyclopropanes: The Influence of Structural and Electronic Properties on the Reactivity. Angew. Chemie Int. Ed. 2019, 58, 1955–1959.
- (51) Veerman, M.; Resendiz, M. J. E.; Garcia-Garibay, M. A. Large-Scale Photochemical Reactions of Nanocrystalline Suspensions: A Promising Green Chemistry Method. Org. Lett. 2006, 8, 2615–2617.
- (52) Hernández-Linares, M. G.; Guerrero-Luna, G.; Pérez-Estrada, S.; Ellison, M.; Ortin, M. M.; Garcia-Garibay, M. A. Large-Scale Green Chemical Synthesis of Adjacent Quaternary Chiral Centers by Continuous Flow Photodecarbonylation of Aqueous Suspensions of Nanocrystalline Ketones. J. Am. Chem. Soc. 2015, 137, 1679–1684.
- (53) Chang, T. Y.; Dotson, J. J.; Garcia-Garibay, M. A. Scalable Synthesis of Vicinal Quaternary Stereocenters via the Solid-State Photodecarbonylation of a Crystalline Hexasubstituted Ketone. Org. Lett. 2020, 22, 8855–8859.
- (54) Kasai, H.; Nalwa, H. S.; Oikawa, H.; Okada, S.; Matsuda, H.; Minami, N.; Kakuta, A.; Ono, K.; Mukoh, A.; Nakanishi, H. A Novel Preparation Method of Organic Microcrystals. *Jpn. J. Appl. Phys.* 1992, 31, L1132–L1134.
- (55) Diazoalkane 6 and acrylates 7a-k were observed in the ¹H NMR analysis of the photolyzed pyrazolines, suggesting a competing retro-1,3-dipolar cycloaddition. This mechanism has been considered as a method to generate diazoalkanes from pyrazolines, though has been studied sparingly. The cyclopropanation chemoselectivity appears to suffer as a result. Another example is noted in reference 56.
- (56) Moiseev, A. G.; Abe, M.; Danilov, E. O.; Neckers, D. C. First Direct Detection of 2,3-Dimethyl-2,3-Diphenylcyclopropanone. J. Org. Chem. 2007, 72, 2777–2784.

- (57) There were no traces of either 6 nor 7a-k from these reactions, suggesting that the retro-1,3-dipolar cycloaddition is a thermally-forbidden, photochemically-allowed, process.
- (58) Shields, D. J.; Karothu, D. P.; Sambath, K.; Ranaweera, R. A. A. U.; Schramm, S.; Duncan, A.; Duncan, B.; Krause, J. A.; Gudmundsdottir, A. D.; Naumov, P. Cracking under Internal Pressure: Photodynamic Behavior of Vinyl Azide Crystals through N2release. J. Am. Chem. Soc. 2020, 142, 18565–18575.
- (59) Commins, P.; Dippenaar, A. B.; Li, L.; Hara, H.; Haynes, D. A.; Naumov, P. Mechanically Compliant Single Crystals of a Stable Organic Radical. *Chem. Sci.* **2021**, *12*, 6188–6193.
- (60) Kim, T.; Zhu, L.; Al-Kaysi, R. O.; Bardeen, C. J. Organic Photomechanical Materials. ChemPhysChem 2014, 15, 400–

- 414.
- (61) Ma, B.; Wu, P.; Wang, X.; Wang, Z.; Lin, H. X.; Dai, H. X. Efficient Synthesis of Spirooxindole Pyrrolones by a Rhodium(III)-Catalyzed C-H Activation/Carbene Insertion/Lossen Rearrangement Sequence. Angew. Chemie -Int. Ed. 2019, 58 (38), 13335–13339.
- (62) Valdéz-Camacho, J. R.; Rivera-Ramírez, J. D.; Escalante, J. Studies and Mechanism of Olefination Reaction in Aryl-Enolates with Paraformaldehyde. *Int. J. Org. Chem.* 2019, 09, 10–22.